Article

Leaf-Scale Study of Biogenic Volatile Organic Compound Emissions from Willow (*Salix* spp.) Short Rotation Coppices Covering Two Growing Seasons

Tomas Karlsson [1,*] , Leif Klemedtsson [2], Riikka Rinnan [3] and Thomas Holst [1]

1   Department of Physical Geography and Ecosystem Science, Lund University, Sölvegatan 12, 223 62 Lund, Sweden; thomas.holst@nateko.lu.se
2   Department of Earth Sciences, University of Gothenburg, Guldhedsgatan 5a, 405 30 Gothenburg, Sweden; leif.klemedtsson@gvc.gu.se
3   Terrestrial Ecology Section, Department of Biology, University of Copenhagen, Universitetsparken 15, DK-2100 Copenhagen, Denmark; riikkar@bio.ku.dk
*   Correspondence: tomas.karlsson@nateko.lu.se

Abstract: In Europe, willow (*Salix* spp.) trees have been used commercially since the 1980s at a large scale to produce renewable energy. While reducing fossil fuel needs, growing short rotation coppices (SRCs), such as poplar or willow, may have a high impact on local air quality as these species are known to produce high amounts of isoprene, which can lead to the production of tropospheric ozone (O_3). Here, we present a long-term leaf-scale study of biogenic volatile organic compound (BVOC) emissions from a Swedish managed willow site with the aim of providing information on the seasonal variability in BVOC emissions during two growing seasons, 2015–2016. Total BVOC emissions during these two seasons were dominated by isoprene (>96% by mass) and the monoterpene (MT) ocimene. The average standardized (STD, temperature of 30 °C and photosynthetically active radiation of 1000 µmol m^{-2} s^{-1}) emission rate for isoprene was 45.2 (±42.9, standard deviation (SD)) µg g_{dw}^{-1} h^{-1}. Isoprene varied through the season, mainly depending on the prevailing temperature and light, where the measured emissions peaked in July 2015 and August 2016. The average STD emission for MTs was 0.301 (±0.201) µg g_{dw}^{-1} h^{-1} and the MT emissions decreased from spring to autumn. The average STD emission for sesquiterpenes (SQTs) was 0.103 (±0.249) µg g_{dw}^{-1} h^{-1}, where caryophyllene was the most abundant SQT. The measured emissions of SQTs peaked in August both in 2015 and 2016. Non-terpenoid compounds were grouped as other VOCs (0.751 ± 0.159 µg g_{dw}^{-1} h^{-1}), containing alkanes, aldehydes, ketones, and other compounds. Emissions from all the BVOC groups decreased towards the end of the growing season. The more sun-adapted leaves in the upper part of the plantation canopy emitted higher rates of isoprene, MTs, and SQTs compared with more shade-adapted leaves in the lower canopy. On the other hand, emissions of other VOCs were lower from the upper part of the canopy compared with the lower part. Light response curves showed that ocimene and α-farnesene increased with light but only for the sun-adapted leaves, since the shade-adapted leaves did not emit ocimene and α-farnesene. An infestation with *Melampsora* spp. likely induced high emissions of, e.g., hexanal and nonanal in August 2015. The results from this study imply that upscaling BVOC emissions with model approaches should account for seasonality and also include the canopy position of leaves as a parameter to allow for better estimates for the regional and global budgets of ecosystem emissions.

Keywords: *Salix* plantation; willow; leaf rust; terpenoids; non-terpenoids; BVOCs; leaf-scale; GC-MS

1. Introduction

The increase in greenhouse gases (GHGs) and the global temperature during the last few decades have resulted in mitigation strategies and climate targets, where the main goal is to keep the average global temperature increase within 1.5–2 °C [1,2] compared

with pre-industrial levels. Together with these climate targets, as declared by the European Union, Sweden also has the goal to have no net emission of GHGs into the atmosphere by 2045 [3]. One option to decrease the use of and dependency on fossil fuel is to use fast-growing biofuel crops, also known as short rotation coppices (SRCs) [4].

Perennial crops are well suited for this purpose and, in particular, willow trees (*Salix* spp.) have been used to produce energy in district heating plants since the 1980s [5]. By using life cycle assessment (LCA), willow as biomass-based energy can reduce the GHG emissions considerably compared with fossil fuel [6]. One of the advantages with willow is the possibility of hybridization and propagation, which makes it easy to develop new varieties for better biomass yield [7]. After initial establishment, the trees grow for between 3 and 5 years before their aboveground biomass is harvested, and plants continue to regrow from their root system for the next harvest cycle. Compared with annual crops, *Salix* trees do not need as much management and fertilization [8]. Current land use of SRC plantations in Sweden is just below 10,000 ha but it has been estimated that this area could expand to 200,000–300,000 ha [9]. Besides the climate change mitigation effects, *Salix* has some other environmental benefits. The plant takes up heavy metals, such as cadmium, from soil [10,11], and can thus be used to clean the soil after application of sludge and wastewater [9,12].

However, *Salix* trees emit high amounts of biogenic volatile organic compounds (BVOCs) [13]. BVOCs are used by plants for signaling, to attract pollinators, and to protect the plants against biotic stress (e.g., herbivory and pathogens) and abiotic stress (e.g., extreme temperatures or pollutants such as ozone (O_3)) [14–19]. However, BVOCs are also important for atmospheric chemistry as they reduce the amount of hydroxyl radicals and thus increase the lifetime of CH_4 [20,21]. The production of O_3 is influenced by the prevailing ratio between VOCs and NO_X [22]. BVOCs could therefore efficiently contribute to the production of tropospheric O_3 in non-NO_X-limited situations [23–25]. Tropospheric O_3 is hazardous as it damages the leaf tissue when entering the stomata, leading to a lower photosynthetic capacity [26,27], but the sink strength of O_3 depends also on the stomatal conductance and thus on the ambient environmental conditions [28,29]. Since O_3 is a GHG, and also could reduce the ability of plants to absorb CO_2, an increase in O_3 might lead to an enhancement in radiative forcing and global warming [30,31]. In addition, BVOCs act as precursors for secondary organic aerosols (SOAs) and enhance cloud condensation nuclei (CCN) production [32–39]. Depending on the properties of the aerosols and the environmental conditions, they can either decrease or enhance global warming [38], but the overall impact of CCN and SOAs is believed to cool the earth [40].

To our knowledge, few studies have investigated the whole emission spectrum of BVOCs from *Salix* [41,42] since the focus has mostly been on isoprene [43,44]. Some studies (e.g., [45]) have investigated emissions from *Salix* at different heights within the canopy. The BVOC emissions from the leaves within the canopy are expected to vary due to the different microclimatic conditions (e.g., temperature and radiation) [45,46], but the difference might be less pronounced for the standardized (STD) emissions.

This study aims to characterize BVOC emissions from *Salix* trees growing in their last year before harvest during the major part of the growing season. Our objectives were to determine seasonal trends in emission rates and spectra, and to assess for differences between leaves growing at different heights within the canopy.

2. Methods

2.1. Site Description

Measurements were done on two plantations in Skrehalla (P1, 58°16′55″ N 12°46′20″ E and P2, 58°17′09″ N 12°45′31″ E), which were located in the southwestern part of Sweden and about 80 km northeast of Gothenburg (Figure S1). The area is flat and the site was mainly surrounded by arable fields. The long-term mean annual temperature was 6.1 °C (1961–1990 in Gendalen, located 16 km from the site) and the annual precipitation was 683 mm (1961–1990 in Grästorp, 7 km from the site) [47]. The soil in the area contained

clay or a silty clay loam with 34–36% clay content, 45–46% silt content, and no organic content (Table 1). Willow trees growing on P1 originated from the species *S. viminalis*. This plantation was established in 1994 and the last time the trees were harvested was in the beginning of 2013, which means measurements were done during their third growing season in 2015. In total, P1 covered approximately 6 ha. The variety growing on P2 is called Tora and P2 was established in 2003 on an area of approximately 5 ha. The trees on P2 were harvested in spring 2013, which means they were in their fourth growing season in 2016. At both sites, all trees were planted in double rows, separated by 0.75 m and 1.25 m between each double row. The distance between the trees in the row was 0.4 m.

Table 1. Information about the two plantations (P1 and P2) in the study. Size (ha), previous land use, year of establishment, canopy height (m), leaf area index (LAI, $m^2 \, m^{-2}$), soil type and content, treatments, varieties, and yield ($m^3 \, ha^{-1}$).

	P1	P2
Size	6 ha	5 ha
Formerly used for	cereals	*Salix*
Established	1994	2003
Canopy height [1]	4.5 m	7 m
LAI [2]	5.5	4.9
Soil type [3]	silty clay loam	clay loam
Clay content [3]	36%	34%
Silt content [3]	46%	45%
Organic content [3]	0%	0%
Treatments [4]	Fertilized (ca 2×100 kg N ha^{-1})	Fertilized (ca 1×100 kg N ha^{-1})
Varieties	unknown *S. viminalis*	Tora
Last harvest	2013	2013
Yield [5]	ca 200 $m^3 \, ha^{-1}$	ca 200 $m^3 \, ha^{-1}$

[1] P1: Estimated average canopy height after the growing season in 2015. P2: Estimated average canopy height after the growing season in 2016. [2] P1: Simulated maximum LAI in 2013 based on measured height and diameter. P2: Measured maximum LAI in 2016. [3] Taken from SGU [48]. [4] Total number of treatments during the rotation cycle. [5] Yield after four growing years.

2.2. Experimental Setup

Measurements were done with two different setups. First, we used a branch chamber (volume ca 13 L) during repeated campaigns throughout the growing seasons 2015 and 2016. The aim of this setup was to follow the seasonal pattern of BVOC emissions during the two growing seasons.

Second, a photosynthesis system with a leaf chamber ($6 \, cm^2$ leaf area) was used to provide photosynthesis information in parallel to BVOC measurements focusing on the light response.

2.2.1. Branch Chamber Setup

The branch chamber used was a cylindrical construction made of PFA and stainless steel covered with a thin transparent PFA film [49–51]. At the beginning of each campaign, the tip (ca 30 cm long) of a shoot from one *Salix* tree was carefully inserted into the chamber the day before measurements started, avoiding any disturbance of the leaves. The chamber was left open on one end when not in use (i.e., during night). Every day before the measurements started, the chamber lid was closed, and the chamber was flushed with purge air for one hour. After this procedure, the branch chamber was used as a dynamic chamber with a continuous purge flow of 3–4 $l \times min^{-1}$, leading to a residence time of ca 4 min for the air within the chamber.

In 2015, only one branch chamber was used. Starting in June 2016, two identical sets of branch chambers were used in parallel at different canopy heights. Each campaign, two trees standing next to each other were chosen for the branch chamber measurements. Prevailing conditions of temperature (T, °C) and relative humidity (RH) were measured both inside and outside the branch chamber (CS215, Campbell Scientific, UT, USA). Pho-

tosynthetically active radiation (PAR, µmol m^{-2} s^{-1}) was measured close to the chamber and at canopy level (Li-190, LI-COR, Lincoln, NE, USA). The data were recorded on a data logger (CR1000, Campbell Scientific, Logan, UT, USA) every 10 sec and stored as 1 min averages.

2.2.2. Light Response Curves and Photosynthesis Rates

Besides the branch chamber, a portable photosynthesis system (LI-6400XT, LI-COR, NE, USA) was used in 2016 to provide photosynthesis information in parallel with BVOC measurements from individual *Salix* leaves [42,46,50,52]. The leaf chamber has a capacity to measure leaves with an area up to 6 cm^2 (2 × 3 cm^2) and the measurements were done on the middle part of the leaves to obtain the maximum area of the leaves. The flow rate into the leaf chamber was set to 500 µmol s^{-1} (ca 0.7 L min^{-1}). The leaf chamber was equipped with a LED source (6400-02B). This photosynthesis system made it possible to control the PAR, T, RH, and carbon dioxide (CO_2) concentration within the leaf chamber. Temperature and CO_2 were set to ambient conditions (20–25 °C and 400 ppm), while PAR was set to increase between 0 and 1500 µmol m^{-2} s^{-1} in six steps (0, 150, 300, 450, 600, 1000, and 1500 µmol m^{-2} s^{-1}) to obtain light response curves. Relative humidity was regulated to match ambient values and ranged mainly from 30% to 70%. Net assimilation rate (A, µmol CO_2 m^{-2} s^{-1}), transpiration (Tr, mmol H_2O m^{-2} s^{-1}), and stomatal conductance (g$_s$, mol H_2O m^{-2} s^{-1}) were measured with the Li-6400XT, and water use efficiency (WUE, mmol CO_2 mol^{-1} H_2O) was then calculated by dividing A by Tr.

2.3. BVOC Sampling

BVOC sampling was based on adsorbent cartridges containing Tenax TA (a porous organic polymer) and Carbograph 1TD (graphitized black carbon (C)) (Markes International Ltd., Mid Glamorgan, UK). Prior to sampling, all cartridges were conditioned. In this process, N_2 is used as a carrier gas while the cartridges are heated up to 300 °C, which empty the cartridges from possible contamination.

Air from the dynamic chamber was pulled through an adsorbent cartridge for 20 min per sample at a flow rate of 200 mL min^{-1} using a flow-controlled pump (Pocket Pump, SKC Ltd., Dorset, UK), leading to a total sample volume of 4 L. In the case of the leaf chamber, the photosynthesis system had been modified with a trace-gas tube connection after the outlet of the leaf chamber [42,46,50,52]. This way, BVOC samples could be taken in parallel to the on-going photosynthesis measurements.

To provide VOC-free and O_3-free air into the branch chamber, air entering the branch chamber was passed through a hydrocarbon trap (Alltech, Associates Inc., Chicago, IL, USA), which contained activated C and a MnO_2-coated copper mesh. The hydrocarbon trap was also attached to the intake of the photosynthesis system. For the branch chamber, background samples of the purge air entering the chamber were taken every day, while blank samples from the empty leaf chamber were taken after the last light intensity (1500 µmol m^{-2} s^{-1}) measurement.

During the campaigns, BVOC samples were taken during day time (8:00–18:00). In the case of the leaf chamber, measurements started one hour after the leaf was inserted to avoid potential stress-induced BVOCs from physical handling [42,52]. When a new light level was set, 30 min passed before the BVOC sampling started so the leaf had time to adapt to the new condition [52]. After sampling, the cartridges were sealed with Teflon-coated brass caps and stored at 3 °C until analysis. After each campaign was finished, the sampled leaves were harvested and dried at 75 °C for two days to measure the dry weight.

In total, 754 samples were taken on 35 trees during 15 campaigns between July 2015 and October 2016, and the campaigns were in general 2–5 days (Table 2). Due to setup and instrumental failure, 26 samples were missing in 2015 and 65 in 2016. Campaigns performed in 2015 were all on P1 except the last one in September, where the first day was on P1 (P1* in Table 2, the star means another variety) and the last two days were on P2. This change was due to a rust outbreak of a fungi (*Melampsora* spp.). Signs of

the infestation were seen in July, and by mid-September most of the trees had shed their leaves (Figure S2). Leaves with the least damage were chosen, but more or less all trees were equally affected. All the campaigns performed in 2016 were done at P2. No signs of *Melampsora* were observed on Tora but leaf-feeding beetles (*Phratora vulgatissima*) damaged the leaves, especially higher up in the canopy. On account of *P. vulgatissima*, undamaged leaves were hard to find, at least in the uppermost part of the canopy, from July onward (Figure S3).

Table 2. All campaigns done in 2015 and 2016 with branch and leaf chambers. Two different plantations (P1 and P2) were studied and new trees were studied each campaign. The star (P1*) means that another variety was measured at this site compared with the rest of the campaigns on P1. Height levels were z_L (up to ca 70% of the total canopy height (TCH)), z_M (up to ca 70% of the TCH but growing at the edge of the plantation), and z_H (heights above z_L). z/H means the ratio between the measured leaves (z) and the canopy height (H).

			Branch Chamber			
Campaign No.	**Time**	**Relative Canopy Height (z/H)**	**Height Group**	**Samples**	**Trees**	**Plantation**
1	2015: 16–17 July	1.00	z_H	8	1	P1
2	2015: 28–31 July	1.00	z_H	30	1	P1
3	2015: 4–7 Aug.	1.00	z_H	28	1	P1
4	2015: 18–21 Aug.	1.00	z_H	31	1	P1
5	2015: 1–4 Sep.	0.85	z_H	31	1	P1
6	2015: 8 and 10–11 Sep.	0.35; 0.80	z_M; z_H	4; 10	2	P1* & P2
				Tot: 142	Tot: 7	

			Branch Chamber			
Campaign No.	**Time**	**Relative Canopy Height (z/H)**	**Height Group**	**Samples**	**Trees**	**Plantation**
1	2016: 4–5 May	0.40	z_M	14	1	P2
2	2016: 24 May	0.75	z_H	6	1	P2
3	2016: 6–10 June	0.30; 0.75	z_M; z_H	39; 10	2	P2
4	2016: 19–23 June	0.30; 0.75	z_M; z_H	39; 40	2	P2
5	2016: 11–15 July	0.30; 0.80	z_M; z_H	36; 36	2	P2
6	2016: 26–29 July	0.70; 0.90	z_M; z_H	32; 30	2	P2
7	2016: 15–17 Aug.	0.55; 0.90	z_M; z_H	20; 12	2	P2
8	2016: 6–9 Sep.	0.65; 0.90	z_M; z_H	30; 28	2	P2
9	2016: 10–13 Oct.	0.50; 0.95	z_M; z_H	29; 26	2	P2
				Tot: 427	Tot: 16	

			Leaf Chamber			
Campaign No.	**Time**	**Relative Canopy Height (z/H)**	**Height Group**	**Samples**	**Trees**	**Plantation**
5	2016: 11–15 July	0.15; 0.15; 0.40	z_M; z_M; z_M	7; 7; 4	3	P2
6	2016: 26–29 July	0.15; 0.60; 0.80; 0.80	z_M; z_L; z_H; z_H	7; 7; 7; 7	3	P2
7	2016: 15–17 Aug.	0.20; 0.65; 0.90	z_M; z_L; z_H	6; 7; 7	3	P2
8	2016: 6–9 Sep.	0.65; 0.20; 0.95; 0.95	z_L; z_M; z_H; z_H	7; 7; 7; 7	3	P2
				Tot: 94	Tot: 12	

The heights of the measurements were divided into three categories. The lower height (z_L) included leaves that were below or in the lower part of canopy (up to ca 70% of the total canopy height (TCH)) and growing within the plantation. The higher height (z_H) included leaves above z_L (>70% of TCH) and growing in a more sun-adapted environment compared with the shade-adapted leaves in z_L. Trees growing at the edge that were <70% of the TCH were classified as middle (z_M) because they were expected to be more sunlit than if they grew within the plantation. The canopy height (H) was measured as the average height for the trees that were growing just next to the leaves, which the BVOC

emissions were measured from, as these trees were responsible for the light conditions at the measured leaves. All measurements during 2015 were done on z_H except for the last campaign. Measurements with the branch chambers in 2016 were done at the edge of P2, while the measurements with the leaf chamber were done both on the edge and within P2.

2.4. Gas Chromatography–Mass Spectrometry and Data Processing

All samples were analyzed by thermal desorption (UNITY2 thermal desorber, Markes International Ltd., Mid Glamorgan, UK) in combination with an ULTRA autosampler and gas chromatograph–mass spectrometer (GC-MS) (7890A Series GC coupled with a 5975C inert MSD/DS Performance Turbo EI System, Agilent, CA, USA) [42,53]. Separation of BVOCs was done by a HP-5 capillary column (50 m × 0.2 mm, film thickness 0.33 μm) and helium was used as a carrier gas. The oven temperature started at 40 °C for 1 min, was first raised to 210 °C with a rate of 5 °C min^{-1}, and was then raised to 250 °C with a rate of 20 °C min^{-1}. The compounds were analyzed in the program Enhanced Chem-Station (MSD ChemStation E.02.01.1177, Copyright 1989–2010 Agilent Technologies, Inc. Santa Clara, CA, USA) and identified by injected external standards (Table S1) or according to mass spectra in the NIST 8.0 database. To quantify BVOCs for which no specific standard was available, α-pinene was used for monoterpenes (MTs), humulene for sesquiterpenes (SQTs), and toluene for other VOCs. Only sample peaks that had at least twice as strong a signal as the corresponding peaks in background samples were chosen for further analysis.

Two compounds, toluene and butylated hydroxytoluene, were removed from all measurements done by LI-6400XT because they had approximately the same concentration in the background samples as the measurements from the leaves and were therefore assumed to be emitted by this instrument.

The emission rates for the BVOCs were calculated by Equation (1), according to Ortega and Helmig [54]

$$E = (C_2 - C_1) \times Q \times m^{-1}. \tag{1}$$

where E (μg g_{dw}^{-1} h^{-1}) is the emission rate, C_2 (μg L^{-1}) is the BVOC concentration taken from the chamber, C_1 (μg L^{-1}) is the BVOC concentration entering the branch chamber or the BVOC concentration inside the empty leaf chamber, Q (L h^{-1}) is the flow rate of the purge air, and m (g_{dw}) is the dried mass of the leaves contained in the chamber.

A standardization for BVOCs that were both light and temperature dependent was done by Equation (2) according to Guenther et al. [55]. The reason for this standardization was to allow for comparison with other studies, regardless of prevailing environmental conditions. The STD values for T and PAR were 303.15 K and 1000 μmol m^{-2} s^{-1}, respectively. The compounds that were STD with Equation (2) were isoprene, ocimene, and α-farnesene.

$$E = E_S \times C_T \times C_L \tag{2}$$

where E (μg g_{dw}^{-1} h^{-1}) is the actual emission at the measured chamber temperature T (K) and *PAR* (μmol m^{-2} s^{-1}), E_s is the STD emission, and C_T and C_L are dimensionless correction factors for temperature and light defined by Equations (3) and (4).

$$C_L = \frac{\alpha C_{L1} PAR}{\sqrt{1 + \alpha^2 PAR^2}} \tag{3}$$

where α (=0.0027) and C_{L1} (=1.066) are empirical coefficients taken from Guenther et al. [55]

$$C_T = \frac{exp \frac{C_{T1}(T - T_s)}{R T_s T}}{1 + exp \frac{C_{T2}(T - T_M)}{R T_s T}} \tag{4}$$

where C_{T1} (=95,000 J mol^{-1}), C_{T2} (=230,000 J mol^{-1}), and T_M (=314 K) are empirical coefficients [55]. R (=8.314 J K^{-1} mol^{-1}) is the universal gas constant and T_s (=303.15 K) is the standard temperature.

For compounds that are temperature, but not light, dependent, the STD emission can be calculated with the temperature-dependent Equation (5), which was used on all terpenoids except isoprene, ocimene, and α-farnesene.

$$E = E_S \times e^{\beta(T-T_s)} \tag{5}$$

where E is the actual emission rate ($\mu g\ g_{dw}^{-1}\ h^{-1}$) at temperature T (K), E_s ($\mu g\ g_{dw}^{-1}\ h^{-1}$) is the STD emission rate at the standard temperature T_s (=303.15 K), and β (=0.09 K^{-1} for MTs and 0.17 K^{-1} for SQTs) is an empirical constant [55,56].

Fitted net assimilation curves were done by using Smith's equation, Equation (6) [57]

$$A = \frac{\alpha_A PAR}{\sqrt{1 + \frac{\alpha_A^2 PAR^2}{A_{max}^2}}} - A_d \tag{6}$$

where A is net assimilation ($\mu mol\ CO_2\ m^{-2}\ s^{-1}$), α_A is the initial quantum yield (mol mol^{-1}), A_d is dark respiration ($\mu mol\ CO_2\ m^{-2}\ s^{-1}$), and A_{max} is net assimilation at the maximum PAR (1500 $\mu mol\ m^{-2}\ s^{-1}$).

The statistical tests were performed with a Kruskal–Wallis test at a significance level of 0.05 when comparing emissions between different heights since the data did not have a Gaussian distribution. The optimized parameters for the fitted light response curves were determined by minimizing the difference between measured and simulated emissions according to a root mean square procedure.

3. Results

3.1. BVOC Emissions from Salix

The total number of detected peaks found during GC-MS analysis was 39 (Table S2), whereof 37 could be identified and the remaining were named as unknown. The average total BVOC emission from all measurements in 2015 and 2016 was 24.4 ($\pm$5.8, standard deviation (SD)) $\mu g\ g_{dw}^{-1}\ h^{-1}$. Isoprene made up more than 96% of the total emission and had an average emission rate of 23.5 ($\pm$28.1) $\mu g\ g_{dw}^{-1}\ h^{-1}$ (Table 3). The corresponding STD isoprene emission rate was 45.2 ($\pm$42.9) $\mu g\ g_{dw}^{-1}\ h^{-1}$.

The average MT emission rate was 0.163 ($\pm$0.117) $\mu g\ g_{dw}^{-1}\ h^{-1}$, which was 0.7% of the total BVOC emission. Nine MTs were detected: allo-ocimene, α-pinene, eucalyptol, limonene, linalool, myrcene, ocimene, p-cymene, and 3-carene. Except in October, ocimene was the dominant MT (0.137 $\pm$ 0.321 $\mu g\ g_{dw}^{-1}\ h^{-1}$) and more than 17 times higher than the second most emitted MT, which was limonene (0.008 $\pm$ 0.042 $\mu g\ g_{dw}^{-1}\ h^{-1}$). The total STD MT emission rate was 0.301 ($\pm$0.201) $\mu g\ g_{dw}^{-1}\ h^{-1}$. The group with the lowest emission rate among the terpenoids was SQTs with an average emission of 0.035 ($\pm$0.062) $\mu g\ g_{dw}^{-1}\ h^{-1}$, which resulted in a contribution of ca 0.1% to the total average BVOC emission. Four SQTs were observed: α-farnesene, caryophyllene, humulene, and nerolidol. The highest average emission rates were seen for caryophyllene (0.011 $\pm$ 0.031 $\mu g\ g_{dw}^{-1}\ h^{-1}$) and humulene (0.010 $\pm$ 0.090 $\mu g\ g_{dw}^{-1}\ h^{-1}$). The average STD emission of SQTs was 0.103 ($\pm$0.249) $\mu g\ g_{dw}^{-1}\ h^{-1}$.

Non-terpenoid compounds were grouped as other VOCs and their classification can be seen in Tables 3 and S2. The most abundant among the identified other VOCs were cyclopentenyl acetylene (0.083 $\pm$ 0.205 $\mu g\ g_{dw}^{-1}\ h^{-1}$), benzaldehyde (0.065 $\pm$ 0.163 $\mu g\ g_{dw}^{-1}\ h^{-1}$), hexanal (0.064 $\pm$ 0.320 $\mu g\ g_{dw}^{-1}\ h^{-1}$), nonanal (0.061 $\pm$ 0.147 $\mu g\ g_{dw}^{-1}\ h^{-1}$), and 2-ethylhexanoic acid (0.059 $\pm$ 0.252 $\mu g\ g_{dw}^{-1}\ h^{-1}$).

Table 3. Average measured (E) and standardized (E_S) emission rates ($\mu g\ g_{dw}{}^{-1}\ h^{-1}$, $n = 663$) from all measurements for the most abundant biogenic volatile organic compounds (BVOCs) in each group. Numbers in parentheses are standard deviation (SD, $\mu g\ g_{dw}{}^{-1}\ h^{-1}$). No standardization was made for other VOCs (−).

BVOC	E ($\mu g\ g_{dw}{}^{-1}\ h^{-1}$)	E_S ($\mu g\ g_{dw}{}^{-1}\ h^{-1}$)
isoprene	23.5 (28.1)	45.2 (42.9)
Total MTs	0.163 (0.117)	0.301 (0.201)
ocimene	0.137 (0.321)	0.255 (0.540)
limonene *	0.008 (0.042)	0.014 (0.081)
p-cymene	0.006 (0.042)	0.011 (0.069)
linalool	0.006 (0.017)	0.010 (0.035)
α-pinene	0.003 (0.021)	0.005 (0.034)
3-carene *	0.002 (0.019)	0.004 (0.040)
Total SQTs	0.035 (0.062)	0.103 (0.249)
caryophellene [†]	0.011 (0.031)	0.024 (0.080)
humulene	0.010 (0.090)	0.040 (0.409)
α-farnesene [†]	0.009 (0.062)	0.017 (0.125)
Total other VOCs	0.751 (0.159)	−
cyclopentyl acetylene [§]	0.083 (0.205)	−
benzaldehyde (benzenoid)	0.065 (0.163)	−
hexanal (aldehyde)	0.064 (0.320)	−
nonanal (aldehyde)	0.061 (0. 147)	−
2-ethylhexanoic acid [§] (carboxylic acid)	0.059 (0.252)	−
pentanal [§] (aldehyde)	0.037 (0.226)	−
decanal [§] (aldehyde)	0.036 (0.148)	−
octanal (aldehyde)	0.030 (0.105)	−
2-methylbutane [§] (alkane)	0.027 (0.105)	−
2-pentanone [§] (ketone)	0.026 (0.208)	−

* These MTs were quantified with α-pinene as the injected standard in GC-MS. [†] These SQTs were quantified with humulene as the injected standard in GC-MS. [§] These other VOCs were quantified with toluene as the injected standard in GC-MS.

3.2. Seasonality of BVOC Emissions Measured with Branch Chambers

3.2.1. Isoprene

The emission rates for isoprene changed mostly according to prevailing T and PAR values. The average STD isoprene emission from P1 in 2015 was 59.3 ($\pm$44.5) $\mu g\ g_{dw}{}^{-1}\ h^{-1}$, where the corresponding average chamber T (T_C) and chamber PAR (PAR_C) were 24.9 ($\pm$ 5.4) °C and 462 ($\pm$296) $\mu mol\ m^{-2}\ s^{-1}$, respectively. Most of the measured isoprene emissions that varied between 92.0 and 153.2 $\mu g\ g_{dw}{}^{-1}\ h^{-1}$ during 2015 occurred in the middle of July and during the second half of August. The chamber T was high (>27.5 °C) and PAR_C varied from 304 to 1654 $\mu mol\ m^{-2}\ s^{-1}$ for these isoprene emissions (Figure 1A–C). The measured emission peaked (153.2 $\mu g\ g_{dw}{}^{-1}\ h^{-1}$) in July and the STD emission peaked (177.6 $\mu g\ g_{dw}{}^{-1}\ h^{-1}$) in August 2015.

With more unsteady weather conditions and under cloudy conditions and even rain, low emissions of isoprene (1.6–7.0 $\mu g\ g_{dw}{}^{-1}\ h^{-1}$) were observed even during the peak growing season in July and August 2015 due to low PARc values (<200 $\mu mol\ m^{-2}\ s^{-1}$). In particular, in the beginning of September when Tc was <15 °C and PARc was <160 $\mu mol\ m^{-2}\ s^{-1}$, the emission rates only reached up to 0.1 $\mu g\ g_{dw}{}^{-1}\ h^{-1}$. In addition, the leaves were damaged in September due to the infestation of *Melampsora* on P1.

The seasonal trend for measured and STD isoprene emissions in 2016 showed an increase from spring to summer; thereafter, it decreased from late summer to mid-autumn. The average STD isoprene emission in 2016 was 30.6 ($\pm$26.7) $\mu g\ g_{dw}{}^{-1}\ h^{-1}$ and the average T_C and PAR_C were 23.2 ($\pm$7.6) °C and 521 ($\pm$444) $\mu mol\ m^{-2}\ s^{-1}$. The measured isoprene emission varied from 50.1 to 143.7 $\mu g\ g_{dw}{}^{-1}\ h^{-1}$ between June and August but
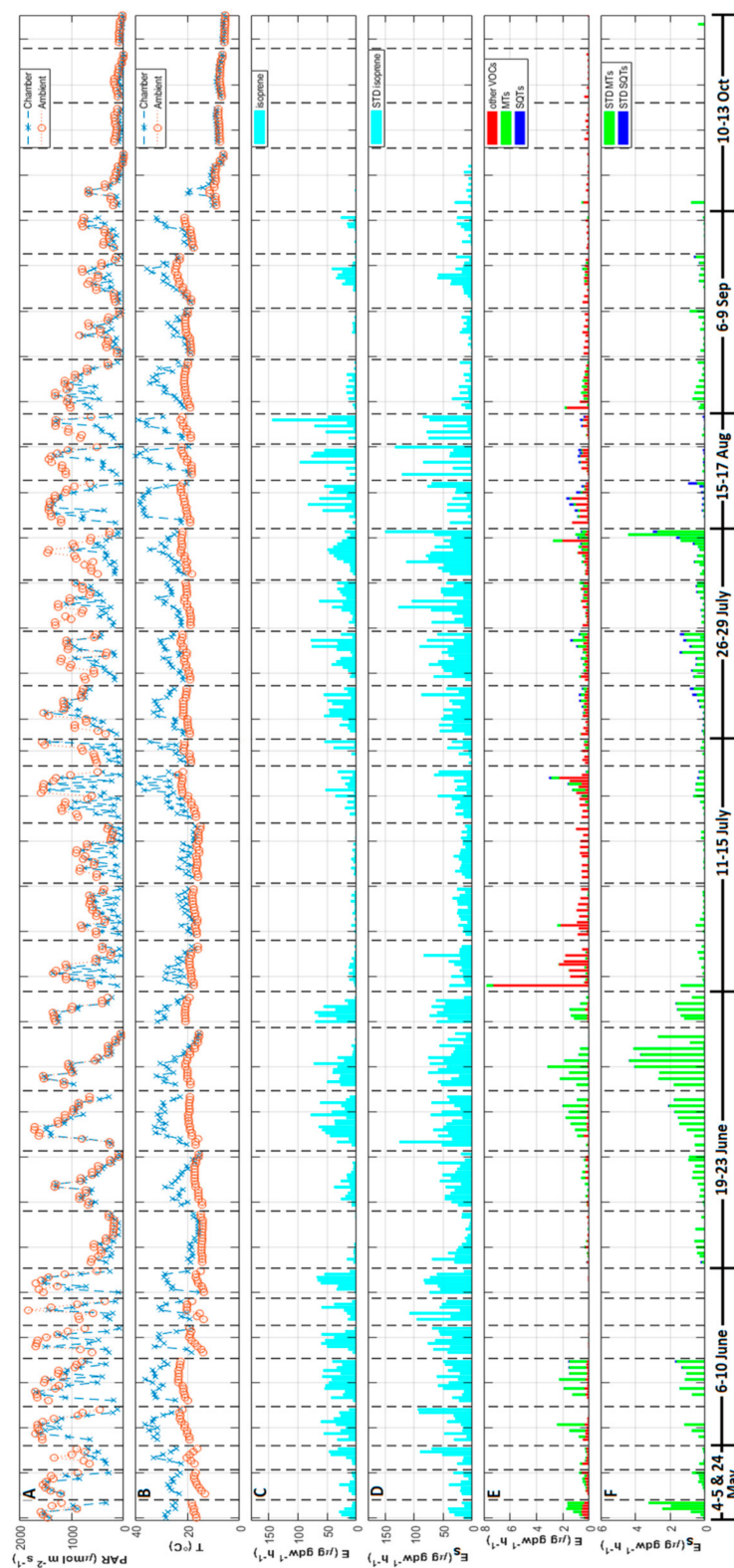
emissions up to 46.5 µg g_{dw}^{-1} h^{-1} were already observed in May (Figure 2C). All measured isoprene emission rates >50 µg g_{dw}^{-1} h^{-1} in 2016 had corresponding T_C and PAR_C ranging from 26.8 to 39.9 °C and from 365 to 1518 µmol m^{-2} s^{-1}. The STD isoprene emission peaked (150.0 µg g_{dw}^{-1} h^{-1}) in late July 2016, while the measured isoprene emission peaked (143.7 µg g_{dw}^{-1} h^{-1}) in August. Isoprene emissions were negligible during the last campaign in October, when T_C and PAR_C were low (less than 11 °C and 110 µmol m^{-2} s^{-1}, respectively).
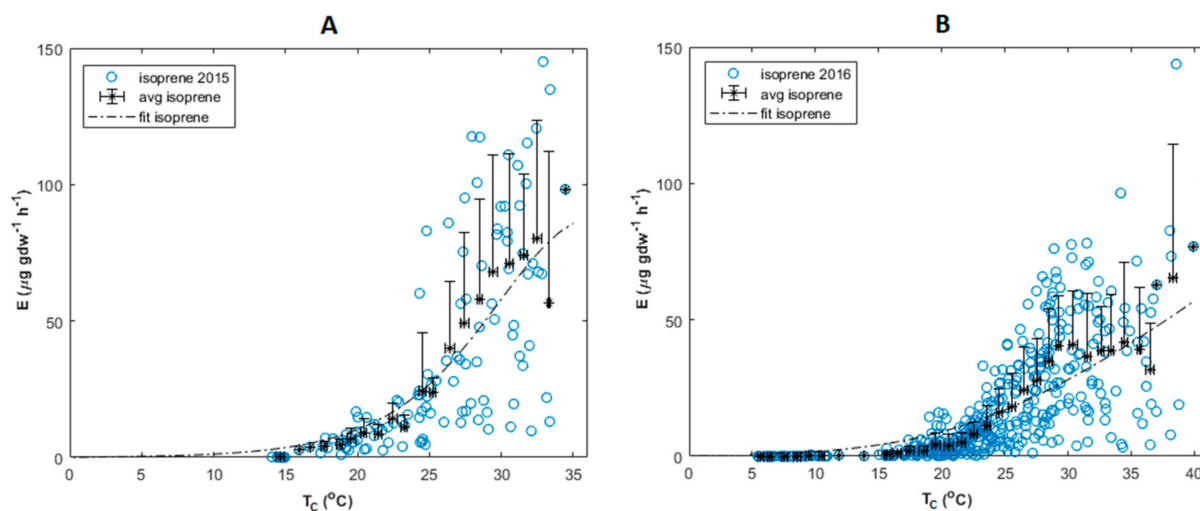
The influence of T_C on the isoprene emission rates showed a stronger exponential increase for the variety on P1 than for Tora on P2 (Figure 3). In particular, when T_C reached above 23 °C, the average emission in 2015 increased faster than during 2016. The steeper response in 2015 was possibly due to the fact that this variety was a stronger emitter of isoprene, but the unexpected lower average emission when T_C varied from 30 to 36 °C in 2016 also reduced the slope of the fitted curve this year.
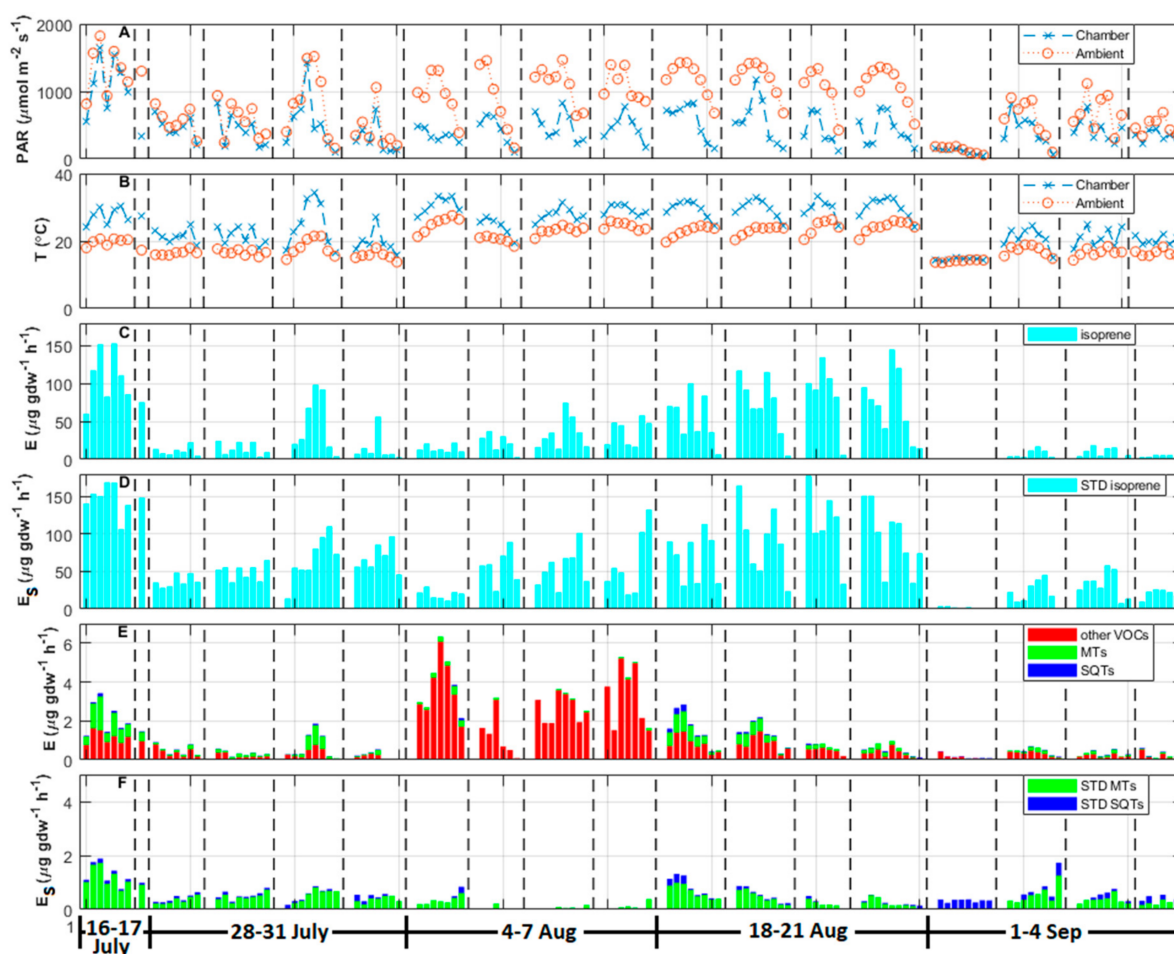
Figure 1. Measurements from P1 in 2015. (**A**) Photosynthetically active radiation (PAR, µmol m^{-2} s^{-1}) values for chamber condition (PAR_C, blue cross and dashed line) and ambient condition (red circle and dotted line). (**B**) Temperature (°C) values for chamber condition (T_C, blue cross and dashed line) and ambient condition (red circle and dotted line). (**C**) Emission rates (µg g_{dw}^{-1} h^{-1}) for isoprene (cyan). (**D**) Standardized (STD) emission rates (µg g_{dw}^{-1} h^{-1}) for isoprene (cyan). (**E**) Emission rates (µg g_{dw}^{-1} h^{-1}) of other VOCs (red), monoterpenes (MTs, green), and sesquiterpenes (SQTs, blue). (**F**) STD emission rates (µg g_{dw}^{-1} h^{-1}) for MTs (green) and SQTs (blue). Vertical dashed lines separate the different days. Each bar represents individual measurements.

Figure 2. Measurements with branch chambers in 2016. (**A**) PAR (μmol m^{-2} s^{-1}) values for chamber condition (PAR$_C$, blue cross and dashed line) and ambient condition (red circle and dotted line). (**B**) Temperature ($^\circ$C) values for chamber condition (T$_C$, blue cross and dashed line) and ambient condition (red circle and dotted line). (**C**) Emission rates (μg g$_{dw}^{-1}$ h^{-1}) for isoprene (cyan). (**D**) Standardized (STD) emission rates (μg g$_{dw}^{-1}$ h^{-1}) for isoprene (cyan). (**E**) Emission rates (μg g$_{dw}^{-1}$ h^{-1}) of other VOCs (red), monoterpenes (MTs, green), and sesquiterpenes (SQTs, blue). (**F**) STD emission rates (μg g$_{dw}^{-1}$ h^{-1}) for MTs (green) and SQTs (blue). Vertical dashed lines separate the different days. Each bar represents individual measurements.

Figure 3. Measured isoprene emissions (blue circles, μg g_{dw}^{-1} h^{-1}), calculated mean emissions + SD (black stars, μg g_{dw}^{-1} h^{-1}), and fitted isoprene emission curves according to Equation (2) versus chamber temperature (T_C, °C) from (**A**) P1 in 2015 and (**B**) P2 in 2016. Values for the parameters can be found in Table S4.

3.2.2. Monoterpenes

The emitted MTs from P1 in 2015 were α-pinene, eucalyptol, linalool, and ocimene. The average STD MT emission was 0.365 (±0.151) μg g_{dw}^{-1} h^{-1}. Ocimene was emitted during all campaigns and the highest measured emissions were seen during the first campaign in mid-July (0.409–1.648 μg g_{dw}^{-1} h^{-1}) and the fourth campaign in mid-August (0–0.932 μg g_{dw}^{-1} h^{-1}). Ocimene contributed with ca 93–100% to the average STD MT emission rate during all campaigns in 2015 (Table S3), and STD emissions of ocimene peaked (1.631 μg g_{dw}^{-1} h^{-1}) in July. α-pinene was the second most abundant MT in 2015, with the STD emission ranging from 0 to 0.076 μg g_{dw}^{-1} h^{-1}, but α-pinene was not observed in September 2015. The total average STD MT emission decreased from 0.580 (±0.292) μg g_{dw}^{-1} h^{-1} in July to 0.286 (±0.182) μg g_{dw}^{-1} h^{-1} in September and a similar trend was seen for the measured average total MT emission.

More MTs were emitted from P2 in 2016. Except for the MTs mentioned above, allo-ocimene, limonene, myrcene, p-cymene, and 3-carene were also observed. The average STD emission of MTs was 0.281 (±0.222) μg g_{dw}^{-1} h^{-1}. Like in 2015, ocimene dominated over the other MTs in 2016 but with higher measured (0–2.930 μg g_{dw}^{-1} h^{-1}) and STD emission rates (0–4.277 μg g_{dw}^{-1} h^{-1}). The measured emission peaked in June and the STD emission peaked in July. Instead of α-pinene, linalool was the second most abundant MT in 2016. The highest measured (0–0.206 μg g_{dw}^{-1} h^{-1}) and STD (0–0.335 μg g_{dw}^{-1} h^{-1}) emissions of linalool occurred in May, and together with ocimene they contributed with more than 97% to the STD MT emission in May. Throughout the rest of the season in 2016 and until September, they contributed with ca 95–99% to the average STD MT emission. Myrcene and allo-ocimene were only seen in June. The STD MT emission during 2016 was highest in May (0.590 ± 0.306 μg g_{dw}^{-1} h^{-1}) followed by June (0.488 ± 0.330 μg g_{dw}^{-1} h^{-1}), and lowest in October (0.022 ± 0.028 μg g_{dw}^{-1} h^{-1}). This pattern was also observed for the measured average total MT emission, which is in line with the MT emission trend in 2015.

3.2.3. Sesquiterpenes

The average STD emission of SQTs from P1 in 2015 was 0.082 (±0.060) μg g_{dw}^{-1} h^{-1}. Caryophyllene had the highest emission rate among the SQTs in 2015 and the STD emission varied between 0 and 0.478 μg g_{dw}^{-1} h^{-1}. The highest STD emissions occurred in September and caryophyllene was the only emitted SQT this month (Figure 1E and Table S3). The measured SQT emission peaked in the second half of August. α-farnesene had the second highest average emission rate among the SQTs during 2015 and was emitted in July

and August. Measured emissions of α-farnesene (0–0.242 μg g_{dw}^{-1} h^{-1}) were highest in August but STD emissions (0–0.193 μg g_{dw}^{-1} h^{-1}) peaked already in late July.

The average STD SQT emission from P2 in 2016 was 0.012 ($\pm$0.018) μg g_{dw}^{-1} h^{-1} and the same SQTs were observed this year as during 2015. August was the month where both the STD emission (0.054 $\pm$ 0.046 μg g_{dw}^{-1} h^{-1}) and the measured emission (0.084 $\pm$ 0.057 μg g_{dw}^{-1} h^{-1}) peaked during 2016. Caryophyllene dominated between June and August and the STD emission varied from 0 to 0.215 μg g_{dw}^{-1} h^{-1}. It contributed with ca 64–96% to the STD SQT emission during these months. α-farnesene was emitted from July to September with STD emissions between 0 and 0.345 μg g_{dw}^{-1} h^{-1}. It was the only SQT observed in September. Humulene was seen from June to July, where the STD emission ranged from 0 to 0.043 μg g_{dw}^{-1} h^{-1}. No SQTs were emitted in May and October.

3.2.4. Other VOCs

The average emission of other VOCs at P1 in 2015 was 0.937 ($\pm$0.105 μg g_{dw}^{-1} h^{-1}). The highest emissions occurred in the beginning of August and the average emission for this campaign was 2.766 ($\pm$0.186) μg g_{dw}^{-1} h^{-1}, which was several times higher compared with most of the other campaigns in 2015 and 2016 (Figures 1F and 2F). The compounds that contributed most in August were nonanal (0–1.570 μg g_{dw}^{-1} h^{-1}), benzoic acid (0–1.330 μg g_{dw}^{-1} h^{-1}), benzaldehyde (0–0.896 μg g_{dw}^{-1} h^{-1}), decanal (0–0.800 μg g_{dw}^{-1} h^{-1}), octanal (0–0.634 μg g_{dw}^{-1} h^{-1}), and hexanal (0–0.607 μg g_{dw}^{-1} h^{-1}). The emissions of many compounds increased during the August campaign compared with the rest in 2015. Compounds such as nonanal and hexanal increased 4-fold, while benzoic acid increased almost 17-fold. The lowest emissions during 2015 were observed in September.

The average emission of other VOCs in 2016 was 0.279 ($\pm$0.049 μg g_{dw}^{-1} h^{-1}). The majority of the highest other VOC emissions were observed during July and especially during mid-July. The emissions of nonanal and benzaldehyde varied from 0 to 1.060 μg g_{dw}^{-1} h^{-1} and 0 to 0.701 μg g_{dw}^{-1} h^{-1} in July, respectively, but during the other months they were usually less than 0.200 μg g_{dw}^{-1} h^{-1}. Emissions of 2-ethylhexanol also peaked in July (0.974 μg g_{dw}^{-1} h^{-1}). Octanal peaked in July but higher emissions were seen in both May and July (0–0.441 μg g_{dw}^{-1} h^{-1}) compared with the other months (0–0.089 μg g_{dw}^{-1} h^{-1}). Tetradecane was only observed in July and August (0–0.034 μg g_{dw}^{-1} h^{-1}), where it peaked in August, and pentadecane was seen in July, August, and September (0–0.072 μg g_{dw}^{-1} h^{-1}).

3.3. Height Comparison with Branch Chamber Measurements in 2016

The average STD isoprene emission from the middle canopy height z_M (33.6 $\pm$ 28.2 μg g_{dw}^{-1} h^{-1}) did not significantly differ from the upper canopy height z_H (26.7 $\pm$ 24.1 μg g_{dw}^{-1} h^{-1}). The largest difference between z_M and z_H for the STD isoprene emission was observed in August (Tables 4 and 5). Due to *P. vulgatissima*, leaves at z_H were more damaged than at z_M in August, which could be one explanation for the different STD isoprene emissions.

Comparing MT emissions between the heights showed that z_H emitted higher rates of MTs than z_M. The average STD MT emission from z_H was 0.509 ($\pm$0.294) μg g_{dw}^{-1} h^{-1} and ca 5 times higher compared with z_M (0.102 $\pm$ 0.137 μg g_{dw}^{-1} h^{-1}; $p < 0.05$). The only time when the average STD MT emission from z_M exceeded that from z_H was in May and October (Tables 4 and 5). In October, it was difficult to find any intact leaves at z_H (Figure S3). Consequently, the leaves at z_H were not able to emit any observable MTs in October. The number of emitted MT compounds from z_H was also larger compared with z_M, which did not have emissions of myrcene and allo-ocimene. Ocimene was the dominantly emitted MT from both z_M (0–91.9%) and z_H (0–96.8%), and linalool also contributed substantially to the MT emission for z_H (0–81.7%). Limonene (0–50.0%), p-cymene (0–33.3%) and 3-carene (0–25.0%) only had a significant contribution for z_M. The only MTs that were observed in October (α-pinene, 3-carene, and limonene) were emitted from z_M.

Table 4. Emission rates (STD for isoprene, MTs, and SQTs, $\mu g\ g_{dw}^{-1}\ h^{-1}$) and fraction (%) of the total BVOC emission or within the BVOC group (MTs and SQTs) from z_H in 2016. Bottom: average T_C (°C), PAR_C ($\mu mol\ m^{-2}\ s^{-1}$), and the corresponding SD for each month.

2016 z_H.	May	June	July	Aug	Sep	Oct
isoprene	44.8 (99.1%)	32.6 (95.8%)	37.5 (98.3%)	11.1 (97.8%)	18.2 (98.1%)	0.2 (87.3%)
MTs (tot)	0.127 (0.3%)	1.240 (3.6%)	0.371 (1.0%)	0.071 (0.6%)	0.275 (1.5%)	0
α-pinene	0	<0.001 (<0.1%)	0.001 (0.3%)	0.001 (1.4%)	0.001 (0.4%)	0
myrcene	0	<0.001 (<0.1%)	0	0	0	0
3-carene	0.008 (6.3%)	0	<0.001 (0.1%)	0.001 (1.4%)	0	0
ocimene	0.004 (3.2%)	1.200 (96.8%)	0.358 (96.4%)	0.038 (53.6%)	0.257 (93.4%)	0
limonene	0.004 (3.2%)	<0.001 (<0.1%)	0.003 (0.8%)	0	0	0
linalool	0.104 (81.7%)	0.033 (2.7%)	0.007 (1.9%)	0.028 (39.4%)	0.016 (5.8%)	0
p-cymene	0.003 (2.4%)	<0.001 (<0.1%)	<0.001 (0.2%)	0.001 (1.4%)	0	0
allo-ocimene	0	<0.001 (<0.1%)	0	0	0	0
eucalyptol	0.004 (3.2%)	0.004 (0.3%)	0.001 (0.3%)	0.002 (2.8%)	0.001 (0.4%)	0
SQTs (tot)	0	0.010 (<0.1%)	0.043 (0.1%)	0	0.007 (<0.1%)	0
α-farnesene	0	0	0.002 (4.7%)	0	0.007 (100%)	0
humulene	0	<0.001 (10.0%)	0.005 (11.6%)	0	0	0
caryophyllene	0	0.009 (90.0%)	0.036 (83.7%)	0	0	0
other VOCs (tot)	0.262 (0.6%)	0.172 (0.5%)	0.228 (0.6%)	0.176 (1.6%)	0.067 (0.4%)	0.029 (12.7%)
BVOCs (tot)	45.189 (100%)	34.021 (100%)	38.140 (100%)	11.347 (100%)	18.549 (100%)	0.229 (100%)
T_C	26.9 (3.5)	24.5 (6.0)	25.5 (4.8)	31.1 (6.4)	25.7 (4.4)	8.8 (2.9)
PAR_C	521 (149)	727 (494)	629 (365)	833 (445)	313 (235)	96 (126)

Table 5. Emission rates (STD for isoprene, MTs, and SQTs, $\mu g\ g_{dw}^{-1}\ h^{-1}$) and fraction (%) of the total BVOC emission or within the BVOC group (MTs and SQTs) from z_M in 2016. Bottom: average T_C (°C), PAR_C ($\mu mol\ m^{-2}\ s^{-1}$), and the corresponding SD for each month.

2016 z_M	May	June	July	Aug	Sep	Oct
isoprene	23.5 (95.3%)	48.7 (99.8%)	34.0 (97.4%)	60.5 (98.9%)	9.6 (96.0%)	2.8 (93.6%)
MTs (tot)	0.788 (3.2%)	0.005 (<0.1%)	0.147 (0.4%)	0.062 (0.1%)	0.012 (0.1%)	0.042 (1.4%)
α-pinene	0	<0.001 (15.9%)	0.004 (2.7%)	0	0	0.007 (16.7%)
myrcene	0	0	0	0	0	0
3-carene	0.002 (0.3%)	<0.001 (6.2%)	0.005 (3.4%)	0	0.003 (25.0%)	0.014 (33.3%)
ocimene	0.701 (89.0%)	0.003 (55.9%)	0.121 (82.3%)	0.057 (91.9%)	0	0
limonene	0	0	0.001 (0.7%)	0	0.003 (25.0%)	0.021 (50.0%)
linalool	0.071 (9.0%)	0	<0.001 (<0.1%)	0.005 (8.1%)	0	0
p-cymene	0.001 (0.1%)	0.001 (22.0%)	0.006 (4.1%)	0	0.004 (33.3%)	0
allo-ocimene	0	0	0	0	0	0
eucalyptol	0.013 (1.6%)	0	0.010 (6.8%)	0	0.002 (16.7%)	0
SQTs (tot)	0	0	0	0.086 (0.1%)	0	0
α-farnesene	0	0	0	0.021 (24.4%)	0	0
humulene	0	0	0	0.009 (10.5%)	0	0
caryophyllene	0	0	0	0.056 (65.1%)	0	0
other VOCs (tot)	0.359 (1.5%)	0.077 (0.2%)	0.761 (2.2%)	0.531 (0.9%)	0.386 (3.9%)	0.149 (5.0%)
BVOCs (tot)	24.647 (100%)	48.782 (100%)	34.908 (100%)	61.179 (100%)	9.998 (100%)	2.991 (100%)
T_C	25.7 (1.7)	25.4 (5.6)	23.1 (3.9)	31.1 (7.0)	24.3 (4.7)	8.6 (2.5)
PAR_C	1135 (406)	699 (469)	298 (254)	627 (450)	486 (342)	83 (123)

The STD SQT emission from z_H (0.019 ± 0.023 $\mu g\ g_{dw}^{-1}\ h^{-1}$) was almost three times larger than from z_M (0.007 ± 0.018 $\mu g\ g_{dw}^{-1}\ h^{-1}$; $p < 0.05$). The same SQTs were observed at

both heights (α-farnesene, caryophellene, and humulene). Sesquiterpenes were seen from z_H in June, July, and September, but only in August from z_M (Tables 4 and 5). Caryophyllene was the dominantly emitted SQT for z_H (0–90.0%) and z_M (0–65.0%).

The number of other VOCs from z_H (20) was almost the same as from z_M (22) but the average emission from z_M (0.347 $\pm$ 0.061 µg g_{dw}^{-1} h^{-1}) was more than twice as high compared with z_H (0.159 $\pm$ 0.030 µg g_{dw}^{-1} h^{-1}; p <0.05). The highest average emission of other VOCs from z_M occurred during July. The compounds that contributed most to this emission in July were benzaldehyde, cyclopentenyl acetylene, 2-ethylhexanol, nonanal, hexanal, and octanal. The average other VOC emission from z_H was highest in May followed by July. Nonanal, hexanal, octanal, and acetophenone were the dominant other VOCs from z_H during May. The average emission of 2-ethylhexanol was 16 times higher from z_M compared with z_H. Hexanal, benzaldehyde, and octanal were 3–4 times higher from z_M compared with z_H. The other VOC emission from z_H was considerably lower at the end of the growing season whereas z_M still emitted higher amounts during September and October.

3.4. Light Response Curves with Leaf Chamber

Starting in the middle of July 2016 and ending in September, light response curves were measured with a leaf chamber at different heights (Table 2). The average emission of isoprene from z_H was 42.2 ($\pm$31.6) µg g_{dw}^{-1} h^{-1} (or 2.42 $\pm$ 1.69 mgC m^{-2} h^{-1}) and almost twice as high as z_L (22.1 $\pm$ 17.3 µg g_{dw}^{-1} h^{-1} or 1.22 $\pm$ 0.84 mgC m^{-2} h^{-1}). The isoprene emission from z_M (33.6 $\pm$ 30.9 µg g_{dw}^{-1} h^{-1} or 1.58 $\pm$ 1.54 mgC m^{-2} h^{-1}) was in between z_H and z_L but the average T_C and PAR_C for z_M (22.7 $\pm$ 2.4 °C and 497 $\pm$ 451 µmol m^{-2} s^{-1}, respectively) were lower than for z_H (24.9 $\pm$ 0.1 °C and 571 $\pm$ 484 µmol m^{-2} s^{-1}, respectively) and z_L (24.8 $\pm$ 0.1 °C and 571 $\pm$ 484 µmol m^{-2} s^{-1}, respectively). The corresponding STD emissions for these height levels were 96.1 ($\pm$64.6) µg g_{dw}^{-1} h^{-1} (or 5.47 $\pm$ 0.26 mgC m^{-2} h^{-1}) (z_H), 94.1 ($\pm$61.9) µg g_{dw}^{-1} h^{-1} (or 4.55 $\pm$ 3.17 mgC m^{-2} h^{-1}) (z_M), and 51.8 ($\pm$32.9) µg g_{dw}^{-1} h^{-1} (2.88 $\pm$ 1.57 mgC m^{-2} h^{-1}) (z_L). Both the measured and the STD isoprene emission for z_H and z_L were significantly different.

In particular, the response to PAR differed between the height levels under low-light conditions for measured isoprene emissions (Figure 4A). For instance, the slope between 0 and 150 µmol m^{-2} s^{-1} for z_H was 0.140 µg g_{dw}^{-1} h^{-1}/(µmol m^{-2} s^{-1}), while it was 0.058 µg g_{dw}^{-1} h^{-1}/(µmol m^{-2} s^{-1}) for z_L (Table S5). This fast response resulted in isoprene comprising more than 90% of the total BVOC emission already at 150 µmol m^{-2} s^{-1} for z_H (Figure 5B). When comparing the STD isoprene emissions between z_L and z_H, then the slope of the fitted curves differed less for low PAR values (Figure S4 and Table S6).
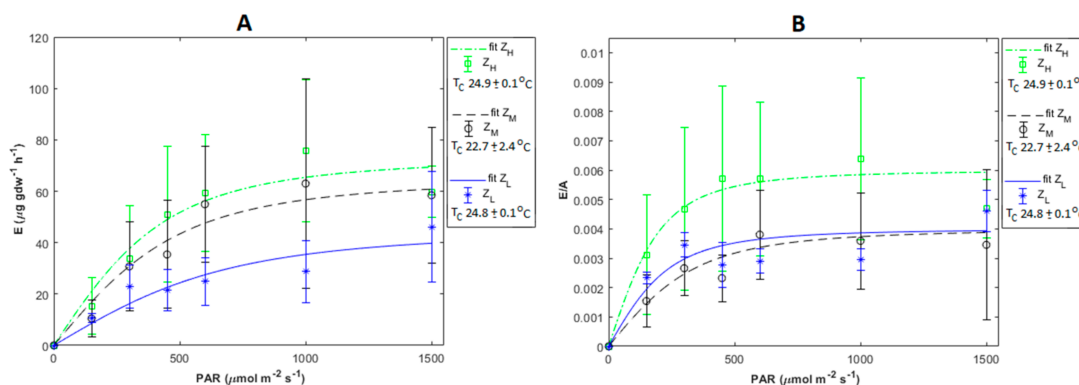
Figure 4. (**A**) Isoprene emission rates (µg g_{dw}^{-1} h^{-1}, mean $\pm$ SD, n = 3–6) and fitted curves for different PAR values (µmol m^{-2} s^{-1}) at different heights using Equation (2). The chamber temperature (T_C, mean $\pm$ SD, n = 3–6) for each height level is included in the legend. Parameter values can be seen in Table S5. (**B**) Ratio between average isoprene emission and net assimilation (unitless, n = 3–6) for different PAR values at different heights. The chamber temperature (T_C, mean $\pm$ SD, n = 3–6) for each height level is included in the legend. The fitted curves are based on Equation (S2) (see Supplementary Materials) and the parameter values can be found in Table S7.
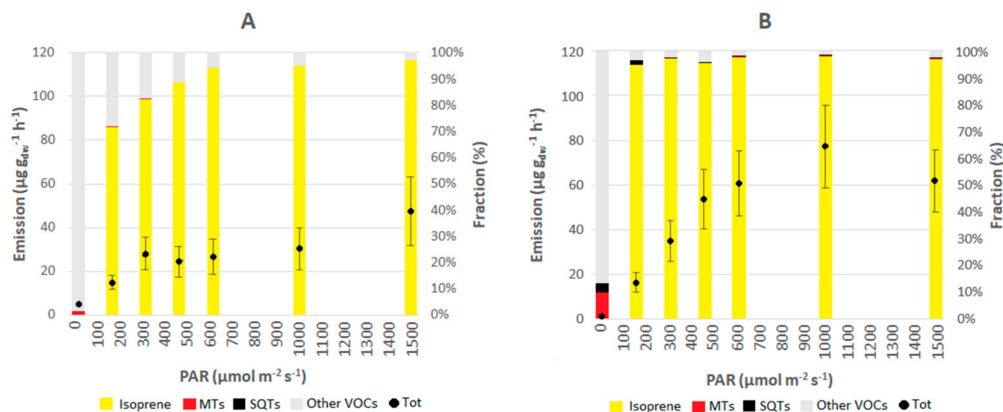
Figure 5. Total emission rates (μg g_{dw}^{-1} h^{-1}, mean $\pm$ SD, black circles and left *y*-axis), and the percentages (stacked bars and right *y*-axis) for the different BVOC groups at different light levels (μmol m^{-2} s^{-1}). (**A**) Lower height (z_L, *n* = 3). (**B**) Higher height (z_H, *n* = 5).

The ratio between isoprene emission and net assimilation (E/A, dimensionless) showed that z_H emitted more of the synthesized C as isoprene relative to the assimilated C, compared with z_M and z_L (Figure 4B). In particular, z_H had the highest E/A ratio when PAR was 1000 μmol m^{-2} s^{-1} and more than 0.6% of the C was emitted as isoprene. For z_M and z_L, this value was less than 0.4% and 0.3%, respectively. z_L was the only height level that increased the E/A ratio from 1000 μmol m^{-2} s^{-1} (ca 0.30%) to 1500 μmol m^{-2} s^{-1} (ca 0.46%).

One MT was seen at z_L (limonene), four at z_H (α-pinene, limonene, p-cymene, and ocimene), and five at z_M (3-carene, α-pinene, limonene, p-cymene, and ocimene). Only ocimene seemed to be influenced by PAR and the average emission of ocimene increased when PAR varied from 300 to 1000 μmol m^{-2} s^{-1} (Figure 6A). The MT emission from z_H (0.078 $\pm$ 0.085 μg g_{dw}^{-1} h^{-1} or 0.004 $\pm$ 0.005 mgC m^{-2} h^{-1}) was almost twice as high as z_L (0.045 $\pm$ 0.029 μg g_{dw}^{-1} h^{-1} or 0.002 $\pm$ 0.002 mgC m^{-2} h^{-1}). The MT fraction was in general lower than 1.0% for all heights and light levels, except when there was no light, due to no isoprene emission (Figures 5A,B and S5).
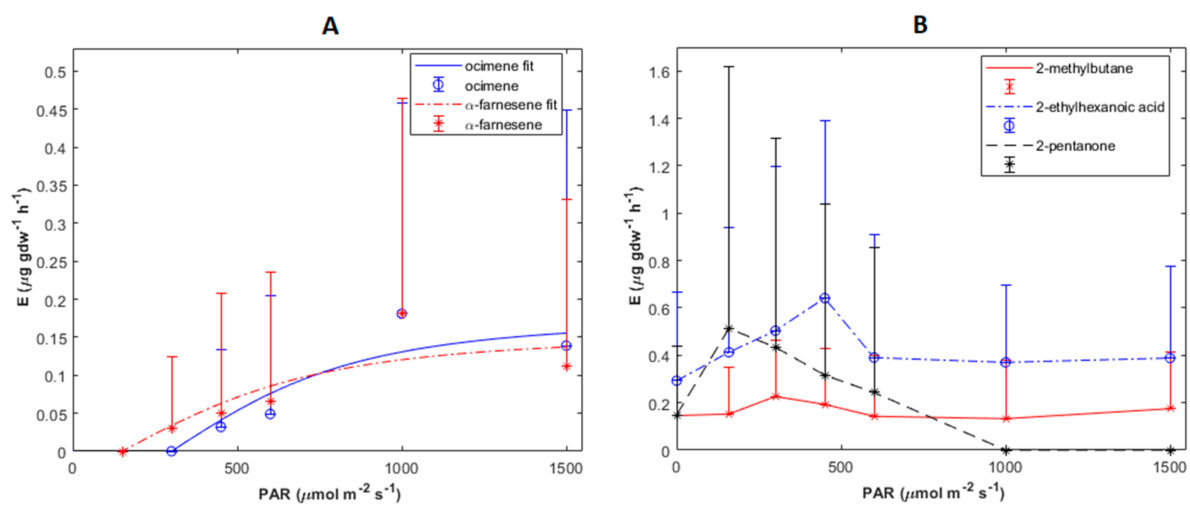
Figure 6. (**A**) Emissions (μg g_{dw}^{-1} h^{-1}, mean + SD, *n* = 11) for ocimene (blue circles) and α-farnesene (red stars) from height levels z_M and z_H at different light levels. Fitted curves have been done by a modified Equation (2), where C_L has been replaced with Equation (S3) for ocimene and Equation (S4) for α-farnesene (see Supplementary Materials for Equations (S3) and (S4) and Table S8 for values). (**B**) Emissions (μg g_{dw}^{-1} h^{-1}, mean + SD, *n* = 7–14) for 2-methylbutane, (red cross), 2-ethylhexanoic acid, (blue circles), and 2-pentanone (black stars) from height levels z_L and z_M.

No SQTs were emitted from z_L. Three SQTs were observed at z_H (α-farnesene, humulene, and nerolidol) and four at z_M (α-farnesene, caryophyllene, humulene, and nerolidol). Average emissions of α-farnesene increased when PAR varied from 150 to 1000 μmol m^{-2} s^{-1} (Figure 6A).

None of the observed other VOCs from the leaf chamber measurements showed a clear relationship with light. However, the emissions of a few compounds seemed to increase or decrease for certain PAR values. The average emission of 2-methylbutane increased from 0.145 ($\pm$0.148) μg g$_{dw}^{-1}$ h^{-1} to 0.226 ($\pm$0.239) μg g$_{dw}^{-1}$ h^{-1} when PAR varied between 0 and 300 μmol m^{-2} s^{-1} and decreased thereafter (Figure 6B). The average emission of 2-ethylhexanoic acid ranged between 0.293 and 0.641 μg g$_{dw}^{-1}$ h^{-1} for the PAR values 0–450 μmol m^{-2} s^{-1}, but the opposite trend was seen for 2-pentanone, the average emission of which decreased from 0.330 to 0 μg g$_{dw}^{-1}$ h^{-1} when PAR increased from 150 to 1000 μmol m^{-2} s^{-1}.

The average net assimilation at the maximum light intensity (1500 μmol m^{-2} s^{-1}) at z_M (21.30 $\pm$ 2.92 μmol CO$_2$ m^{-2} s^{-1}) and z_H (18.10 $\pm$ 4.89 μmol CO$_2$ m^{-2} s^{-1}) was higher than at z_L (12.05 $\pm$ 3.01 μmol CO$_2$ m^{-2} s^{-1}) (Figure 7A and Table 6). The average A values for each light step for z_M and z_H increased all the way up to 1500 μmol m^{-2} s^{-1}, while the average A for z_L leveled out when PAR exceeded 600 μmol m^{-2} s^{-1}. (Figure 7A and Table S9).
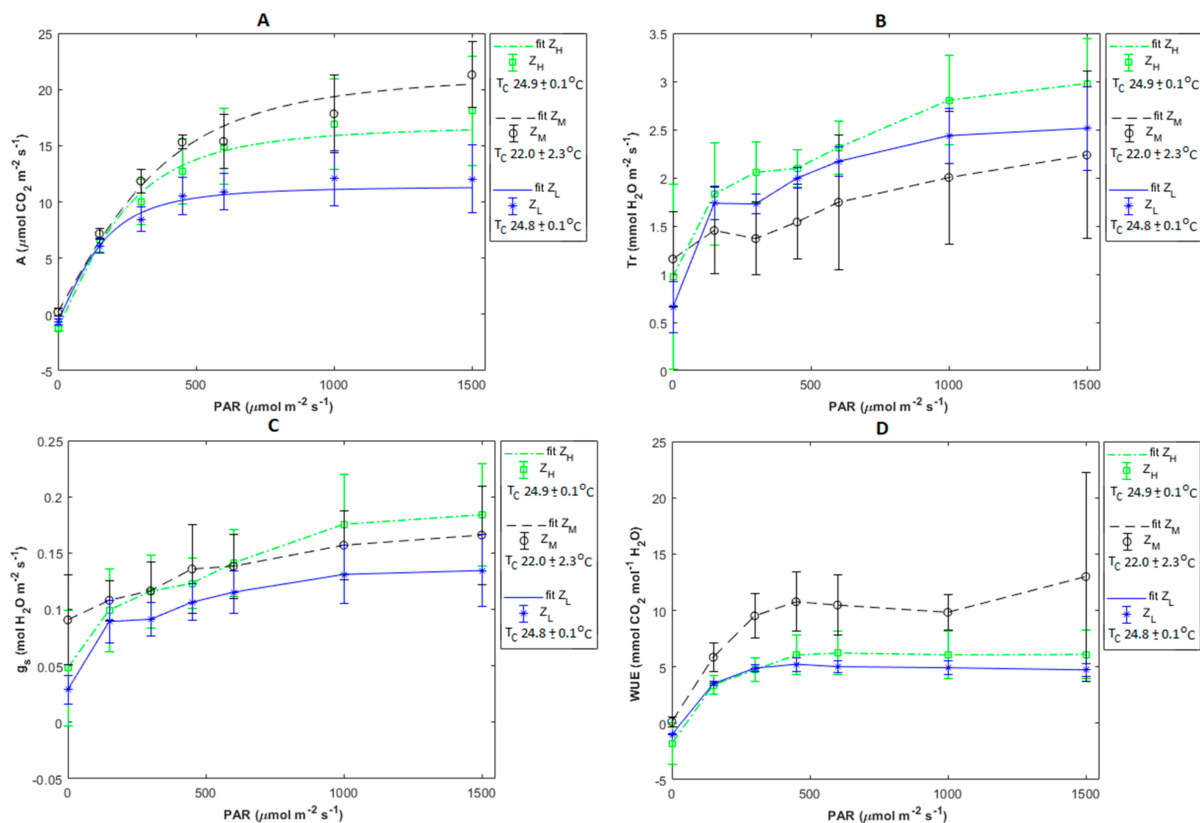
Figure 7. (**A**) Net assimilation (A, mean $\pm$ SD, μmol CO$_2$ m^{-2} s^{-1}, n = 2–6) and fitted curves by using Equation (6) (values of parameters can be seen in Table S10), (**B**) transpiration (Tr, mean $\pm$ SD, mmol H$_2$O m^{-2} s^{-1}, n = 2–6), (**C**) stomatal conductance (g_s, mean $\pm$ SD, mol H$_2$O m^{-2} s^{-1}, n = 2–6), and (**D**) water use efficiency (WUE, mean $\pm$ SD, mmol CO$_2$ mol^{-1} H$_2$O, n = 2–6) for different PAR (μmol m^{-2} s^{-1}) and height levels. The chamber temperature (T$_C$, mean $\pm$ SD, n = 3–6) for each height level is included in all legends.

Transpiration at z_H was higher than at z_M and z_L when there was light (Figure 7B). Stomatal conductance at z_H exceeded g_s at z_M and z_L at light intensities above 600 μmol m^{-2} s^{-1} (Figure 7C). The lower height had the lowest g_s response to PAR but was mainly in between z_H and z_M for Tr. Water use efficiency was similar for z_H and z_L when PAR varied between

0 and 450 μmol m^{-2} s^{-1}; thereafter, z_H increased to ca 6 mmol CO_2 mol^{-1} H_2O while z_L was more or less constant and remained below 5 mmol CO_2 mol^{-1} H_2O (Figure 7D). On the other hand, WUE for z_M was approximately twice as high as for z_H and z_L for 450–1500 μmol m^{-2} s^{-1}.

Table 6. Mean values for net assimilation (A, μmol CO_2 m^{-2} s^{-1}, n = 3–6), transpiration (Tr, mmol H_2O m^{-2} s^{-1}, n = 3–6), water use efficiency (WUE, mmol CO_2 mol^{-1} H_2O, n = 3–6), and stomatal conductance (g_s, mol H_2O m^{-2} s^{-1}, n = 3–6) at 1500 μmol m^{-2} s^{-1} for different height levels. Numbers in parentheses are SD.

PAR = 1500 μmol m^{-2} s^{-1}	Lower (z_L)	Middle (z_M)	Higher (z_H)
A (μmol CO_2 m^{-2} s^{-1})	12.05 (3.01)	21.30 (2.92)	18.10 (4.89)
Tr (mmol H_2O m^{-2} s^{-1})	2.51 (0.43)	2.24 (0.97)	2.98 (0.47)
WUE (mmol CO_2 mol^{-1} H_2O)	4.73 (0.55)	12.99 (9.28)	6.10 (2.13)
g_s (mol H_2O m^{-2} s^{-1})	0.13 (0.03)	0.17 (0.04)	0.18 (0.05)

4. Discussion

4.1. Isoprene Emissions, Net Assimilation, and Water Use Efficiency

As expected, isoprene was the dominant compound throughout the growing season and made up 90–99% of the total BVOC emission, with measured emission rates reaching up to 150 μg g$_{dw}$$^{-1}$ h^{-1}. The STD isoprene emission rate averaged over the whole study (45.2 μg g$_{dw}$$^{-1}$ h^{-1}) is comparable to what has been shown in other studies [13,58,59]. However, the reported range of STD isoprene emission rates is wide [13,59]. In Morrison et al. [59], the STD isoprene emission for unknown *Salix* spp. varieties varied from 0.1 to 15.9 μg g$_{dw}$$^{-1}$ h^{-1} for three different sites in the United Kingdom. In their study, a similar method was used as in this study but since they included the whole year, a lower emission can be expected on account of the low temperature and PAR during the non-peak season. Moreover, the age of the measured trees was not the same in their study (first, second, and third growing season) as in this study (third and fourth growing season). Another study done close to our site reported a ca 6 times lower STD isoprene emission from clones that originated from the same species (*S. viminalis*) as was measured in this study, during peak summer [44]. In their study, a relaxed eddy accumulation technique scaled by foliar mass density was used, which is a different method compared with the methods used in this study and could therefore explain the disparity. In particular, this method includes measurements from the whole canopy, i.e., both sun-exposed and shaded leaves, whereas most leaves in this study were adapted to sunlit conditions. Additionally, emission rates vary within the same species [13], which can explain why the average STD isoprene emission in 2015 was twice as high as in 2016, despite similar T_C and PAR$_C$, since the plantations contained different varieties. According to Karlsson et al. [42], it has been shown that *Salix* varieties growing on SRC fields emit various amounts of isoprene and that the Tora-variety growing on P2 is a low emitter.

The seasonal patterns for isoprene emissions in the two *Salix* varieties we measured in 2015 and 2016 were similar. The highest emission rates typically occurred when weather was warm and sunny. The measurements in 2016 showed that the trees were able to emit high rates of isoprene already in the beginning of May. At this point, the weather had started to become warmer, which resulted in the trees developing small leaves with a light green color. It is well known that isoprene emission is influenced by temperature because of the linkage to the enzyme isoprene synthase [60,61]. In September, measured and STD isoprene emissions during 2015 and 2016 started to decline compared with the former months. In October 2016, isoprene emissions were negligible. The reason for the declining trend is mostly explained by changing weather (2015), and the approaching fall and leaf senescence [62,63]. In particular, all isoprene emissions were <3.0 μg g$_{dw}$$^{-1}$ h^{-1} and most of the samples contained no isoprene during October. Zero emissions of isoprene occurred when T_C was ca 11 °C or lower, and PAR$_C$ <110 μmol m^{-2} s^{-1}, indicating that these values

could be a threshold for isoprene emission during late season for this location and variety. These growing conditions in combination with the leaf damage caused by *P. vulgatissima* explain why the isoprene emissions from z_H were exceptionally low in October since many leaves at z_H were almost gone and more or less only the midrib was left (Figure S3).

The *Melampsora* infestation on P1 likely affected the emission rates. Toome et al. [64] showed that willow trees infected with *Melampsora* reduced their isoprene emission rates by almost 30% and a similar result was observed for *Populus* [65]. Perhaps, the isoprene emissions would have been even higher in 2015 if no *Melampsora* outbreak had occurred.

Measured and STD isoprene emissions from the more sunlit leaves (z_H) exceeded emission rates from shaded leaves (z_L) as expected [45,66,67]. Previous studies have reported a hyperbolic curve for isoprene when PAR increases [55,68,69], which can be linked to the photosynthetic electron transport [69,70], and a similar behavior was observed in this study. Isoprene emissions from sun-adapted leaves at z_H responded faster to increased light, and reached twice as high maximum emission rates. This result is in line with Sharkey et al. [66], who studied isoprene emissions from oak and aspen, and it also points out that large errors can be expected if up-scaled emissions are based on data from only one canopy height [45].

The isoprene emission increased exponentially with temperature but it is hard to state if the optimum temperature was reached in our study. In a subarctic *Salix myrsinites*, isoprene emission increased exponentially across the temperature range of 10–38 °C without reaching a maximum [71]. According to Niinemets et al. [72], the optimum often occurs around 40 °C, suggesting that this could be the same for the varieties in this study. Nevertheless, measurements at higher temperatures are needed to confirm this.

The net assimilation was higher for z_H compared with z_L, but lower than for z_M. An increasing A pattern with canopy height has been reported previously [73,74]. Since also Tr from z_M was below the others, this resulted in a higher WUE for z_M, making these leaves more efficient in their water use than the leaves at z_L and z_H. The E/A ratio at z_H exceeded that at z_L, which means that the light-adapted leaves in the upper part of the canopy lose more C as isoprene than less light-adapted leaves. However, despite the lower isoprene emission rates from the shaded leaves at z_L, they showed a strong increase (ca 50%) in their E/A ratio when PAR increased from 1000 to 1500 µmol m^{-2} s^{-1}. So, even for leaves less acclimatized to sunlight, isoprene serves as a strongly induced compound when the leaves are light-stressed. The leaves that were more sun-adapted (z_H and z_M) did not show this pattern.

Measurements of A and simultaneously emitted BVOCs showed that the trees only used a minor fraction (0.4%) of photosynthetic C for BVOC emission, although compounds with less than five carbon units (i.e., methanol, acetone) were not detectable with the methods used in this study. This ratio is comparable with the results from a study conducted during summer on a spruce forest, where the assimilated C loss on average was approximately 0.3% [75]. For isoprene, the ratio between emitted C and A was similar to what had been found for some species of poplar [76], which are also known to be high isoprene emitters. Only a small percentage of the net carbon assimilation is in general released as BVOCs [77–80] but under stressed conditions, carbon loss can be 7–8% due to increased isoprene emissions [68,81].

The maximum A for the sunlit leaves is in line with results in other studies, which suggest that A for *Salix* trees can vary between 10 to 35 µmol CO_2 m^{-2} s^{-1} [42,82]. The WUE values for z_L and z_H were comparable with the values for Tora reported in Karlsson et al. [42].

The variety Tora in Karlsson et al. [42] had a ca 80% lower STD isoprene emission compared with Tora on P2 when comparing the leaf chamber measurements for sun-adapted leaves. This difference is probably due to the fact that the trees were younger (first and second growing season) in Karlsson et al. [42].

Changing from traditional crops, e.g., wheat, rye, oat, or oilseed rape, which are low emitters of isoprene [59,83–85] to a SRC (e.g., willow) would drastically alter the regional concentration of isoprene and increase the risk of O_3 production near polluted areas [86–88].

4.2. Emissions of Monoterpenes, Sesquiterpenes, and Other Volatile Organic Compounds

The second most emitted compound was ocimene and together with α-pinene, they contributed with more than 95% to the MT emission throughout 2015. In 2016, ocimene dominated over the other MTs, followed by limonene, p-cymene, and linalool. Even if the emission rates of the MTs varied individually during the season, both 2015 and 2016 showed the same trend, where the measured average total emission of MTs decreased across the measurement periods, but occasional higher emissions were still possible in late summer and autumn. Emissions of MTs can be dependent on the season and willow leaves have shown a stronger capacity to emit MTs in the beginning of the growing season close to bud break [59,89]. However, we cannot verify this suggestion as we did not measure in early spring. The most abundant SQTs were caryophyllene, humulene, and α-farnesene. The emissions of these compounds peaked in the second part of the growing season between July and September. No SQTs could be observed during May and October.

Ocimene and α-farnesene were the only terpenes, besides isoprene, that were influenced by PAR. Ocimene was also found to increase with light by Karlsson et al. [42]. Many studies have shown a correlation between terpenes and light [42,90–92]. This similarity with isoprene shows that emissions of some MTs and SQTs could be described by a similar light- and temperature-dependent algorithm developed by Guenther et al. [55] for short-term emissions.

Shade-adapted leaves at z_L emitted less MTs and had lower emission rates than the sun-adapted leaves at z_H but the emissions from z_M were higher than z_H in May and October. The only month when the SQT emission from the lower height (z_M) exceeded that from the higher height level (z_H) was in August. Neither ocimene nor α-farnesene were emitted from z_L, which suggests that the leaves require an adaption to an environment with sufficient sunlight to be able to emit these terpenes. Monoterpenes and SQTs are very reactive and protect the plant against different abiotic and biotic stresses [49,93–100].

Several times higher emissions of other VOCs were observed in August 2015 compared with the other months this year. The compounds responsible for these emission rates (e.g., benzaldehyde, nonanal, octanal, decanal, and hexanal) have been reported to be induced during abiotic and biotic stresses [65,101–104]. Jiang et al. [65] reported induced emissions of nonanal and decanal from *Populus* leaves infested by *Melampsora*. Toome et al. [64] also studied the impact of *Melampsora* and showed that an infection on willow trees resulted in increased emission of some GLVs (e.g., (Z)-3-hexenol and (E)-2-hexenal), as well as (Z)-β-ocimene and (E,E)-α-farnesene. Moreover, Arimura et al. [105] observed stress-induced emissions of (E)-β-ocimene, linalool, and (E,E)-α-farnesene from poplar leaves eaten by caterpillar. The higher emissions of α-farnesene and caryophyllene might have been a consequence of the *Melampsora* infestation (2015) and herbivore insects (2016).

Emissions of other VOCs were larger from the lower canopy height compared with the higher canopy height, but it is difficult to pinpoint the underlying reason. If the leaves were more attractive to leaf-eating insects at the upper canopy, one would expect higher emission rates from this level as a self-defending mechanism [94,106]. On the other hand, the higher emission rates from the lower canopy could be the reason why these beetles strike the upper part. However, one explanation for the difference might be related to how the leaves looked. In July and August, the leaves at the lower height were smaller with a brighter green color compared with the higher height. Further, the damage by *P. vulgatissima* is believed to have reduced the emission from the upper part of the canopy, especially in October.

Most studies have only focused on isoprene and a few other compounds, which usually are most abundant [43,59,107,108]. Even if isoprene is dominant and crucial for air chemistry processes, other compounds might also be of importance. Monoterpenes

constitute a group responsible for particle formation and generation of SOAs [38,109]. Additionally, stress-induced compounds are usually not included (yet) in modeling processes, but biogenic non-terpenoids can contribute with the same magnitude as anthropogenic sources of non-terpenoids to SOA formation and should not be discarded [104].

5. Summary and Conclusions

We studied seasonal trends and canopy height differences for BVOC emissions of willow varieties growing as bioenergy crops on SRC fields. The majority of the measurements in 2015 were done on an unknown variety belonging to *S. viminalis*, while all measurements in 2016 were on the variety Tora. The results from this study confirm that isoprene was the most dominant BVOC during the major part of the growing season. Emissions of MTs, SQTs, and other VOCs were in general only a minor fraction of the total BVOC emission. The prevailing infestation of *Melampsora* (2015) was probably responsible for increased emissions of, e.g., nonanal, hexanal, and caryophyllene.

The emissions of isoprene peaked during summer (in July 2015 and in August 2016) but the leaves had high emissions already in May. The seasonal pattern for SQTs showed that these peaked during summer as well. Emissions of MTs showed a decreasing trend from May to October and the overall terpenoid emission seemed to be substantially lower by the end of the growing season as a consequence of colder weather and proceeding leaf senescence.

Our study suggests that Tora is a better choice when it comes to having a reduced risk for impaired air quality since it emitted ca 50% less isoprene, which can be a source for O_3 and peroxyacetyl nitrate. Nevertheless, *Salix* trees are high emitters of isoprene compared with commercial crops, and an expansion of *Salix* plantations would need to be strategically planned and placed at a sufficiently long distance away from pollution sources to avoid elevated photochemical production of O_3 under high NO_x conditions.

Leaves higher up in the canopy and acclimatized to more sunlight emitted higher rates of isoprene than the leaves growing in the lower and more shaded parts of the canopy. Emissions of MTs were also lower for the leaves in the shaded conditions and no SQT emissions were observed from the shade-adapted leaves. On the contrary, emissions of non-terpenoids were higher from the lower part of the canopy. These results point out that the location within the canopy is one important factor when it comes to emissions of different compounds, particularly those compounds that are dependent on PAR. Hence, to make better estimations of the regional and global BVOC fluxes, models need to adjust for, e.g., the vertical distribution of leaf area within the canopy layer.

Ocimene and α-farnesene were the only compounds, except isoprene, that were influenced by light, suggesting that they can be modeled with a similar algorithm as isoprene.

This study highlights that scaling-up BVOC emissions and basing models on one simplified emission potential for the whole canopy could lead to large errors.

Author Contributions: Conceptualization, T.H. and T.K.; methodology, T.H.; software, T.H.; validation, T.K. and T.H.; formal analysis, T.K.; investigation, T.K.; data curation, T.K., T.H. and R.R.; resources, T.H., R.R. and L.K; writing—original draft preparation, T.K.; writing—review and editing, T.K., R.R., L.K. and T.H.; supervision T.H.; project administration, T.K. and T.H.; funding acquisition, T.H. All authors have read and agreed to the published version of the manuscript.

Institutional Review Board Statement: Not applicable.

Informed Consent Statement: Not applicable.

Data Availability Statement: Data from this study is available from the corresponding author upon reasonable request.

Conflicts of Interest: The authors declare no conflict of interest. The funders had no role in the design of the study; in the collection, analyses, or interpretation of data; in the writing of the manuscript; or in the decision to publish the results.

References

1. *A Policy Framework for Climate and Energy in the Period from 2020 up to 2030*; European Commission: Brussels, Belgium, 2014.
2. IPCC. 2021: Summary for Policymakers. In *Climate Change 2021: The Physical Science Basis. Contribution of Working Group I to the Sixth Assessment Report of the Intergovernmental Panel on Climate Change*; Masson-Delmotte, V., Zhai, P., Pirani, A., Connors, S.L., Péan, C., Berger, S., Caud, N., Chen, Y., Goldfarb, L., Gomis, M.I., et al., Eds.; Cambridge University Press: Cambridge, UK, 2021; In press.
3. Bonde, I.; Kuylenstierna, J.; Bäckstrand, K.; Eckerberg, K.; Kåberger, T.; Löfgren, Å.; Rummukainen, M.; Sörlin, S. *2020-Report of the Swedish Climate Policy Council*; Rapport nr 3; Swedish Climate Policy Council: Stockholm, Sweden, 2020; ISBN 978-91-984671-4-7.
4. Don, A.; Osborne, B.; Hastings, A.; Skiba, U.; Carter, M.S.; Drewer, J.; Flessa, H.; Freibauer, A.; Hyvönen, N.; Jones, M.B.; et al. Land-use change to bioenergy production in Europe: Implications for the greenhouse gas balance and soil carbon. *Glob. Chang. Biol. Bioenergy* **2011**, *4*, 372–391. [CrossRef]
5. Lindegaard, K.N.; Adams, P.W.; Holley, M.; Lamley, A.; Henriksson, A.; Larsson, S.; von Engelbrechten, H.G.; Esteban Lopez, G.; Pisarek, M. Short rotation plantations policy history in Europe: Lessons from the past and recommendations for the future. *Food Energy Secur.* **2016**, *5*, 125–152. [CrossRef]
6. Kimming, M.; Sundberg, C.; Nordberg, Å.; Baky, A.; Bernesson, S.; Norén, O.; Hansson, P.A. Biomass from agriculture in small-scale combined heat andpower plants—A comparative life cycle assessment. *Biomass Bioenerg.* **2011**, *35*, 1572–1581. [CrossRef]
7. Åhman, I.; Larsson, S. *Resistensförädling i Salix för Energiproduktion, SLU*; Institutionen för entomologi, Nr/avsnitt: 2; SLU: Alnarp, Sweden, 1999.
8. Kägi, T.; Deimling, S.; Knuchel, R.F.; Gaillard, G.; Hölscher, T.; Müller-Sämann, K. Environmental impacts of annual and perennial energy crops compared to a reference foo crop rotation. In Proceedings of the Empowerment of the Rural Actors: A Renewal of Farming Systems Perspectives 8th European IFSA Symposium, Clermont-Ferrand, Clermont-Ferrand, France, 6–10 July 2008; pp. 675–681.
9. Fredga, K.; Danell, K.; Frank, H.; Hedberg, D.; Kullander, S. Bioenergy—Opportunities and constraints. In *Energy Committee Report*; Kungliga Vetenskapsakademin: Stockholm, Sweden, 2008.
10. Landberg, T.; Greger, M. Differences in uptake and tolerance to heavy metals in Salix from unpolluted and polluted areas. *Appl. Geochem.* **1996**, *11*, 175–180. [CrossRef]
11. Meers, E.; Vandecasteele, B.; Ruttens, A.; Vangronsveld, J.; Tack, F. Potential of five willow species (Salix spp.) for phytoextraction of heavy metals. *Environ. Exp. Bot.* **2007**, *60*, 57–68. [CrossRef]
12. SOU 2007:36. *Bioenergi från Jordbruket–en Växande Resurs*; Statens Offentliga Utredningar; Edita Sverige AB: Stockholm, Sweden, 2007; ISBN 978-91-38-22751-0.
13. Kesselmeier, J.; Staudt, M. Biogenic volatile organic compounds (VOC): An overview on emission, physiology and ecology. *J. Atmos. Chem.* **1999**, *33*, 23–88. [CrossRef]
14. Dicke, M.; Vet, L.E.M. Plant-carnivore carnivore interactions: Evolutionary and ecological consequences for plant, herbivore and carnivore. In *Herbivores: Between Plants and Predators*; Olff, H., Brown, V.K., Drent, R.H., Eds.; Blackwell Science: Oxford, UK, 1999; pp. 483–520.
15. Llusià, J.; Peñuelas, J. Emission of volatile organic compounds by apple trees in response to spider mite attack and attraction of predatory mites. *Exp. Appl. Acarol.* **2001**, *25*, 65–77. [CrossRef] [PubMed]
16. Dicke, M.; van Poecke, R.M.P.; de Boer, J.G. Inducible indirect defence of plants: From mechanisms to ecological functions. *Basic Appl. Ecol.* **2003**, *4*, 27–42. [CrossRef]
17. Dudareva, N.; Pichersky, E. Metabolic engineering of plant volatiles. *Curr. Opin. Biotechnol.* **2008**, *19*, 1–9. [CrossRef]
18. Laothawornkitkul, J.; Taylor, J.; Paul, N.; Hewitt, C. Biogenic volatile organic compounds in the Earth system. *New Phytol.* **2009**, *183*, 27–51. [CrossRef]

19. Possell, M.; Loreto, F. The role of volatile organic compounds in plant resistance to abiotic stresses: Responses and mechanisms. In *Biology, Controls and Models of Tree Volatile Organic Compound Emissions*; Niinemets, Ü., Monson, R.K., Eds.; Tree Physiology; Springer: Berlin/Heidelberg, Germany, 2013; Volume 5, pp. 209–235.

20. Folberth, G.A.; Hauglustaine, D.A.; Lathière, J.; and Brocheton, F. Interactive chemistry in the Laboratoire de Météorologie Dynamique general circulation model: Model description and impact analysis of biogenic hydrocarbons on tropospheric chemistry. *Atmos. Chem. Phys.* **2006**, *6*, 2273–2319. [CrossRef]

21. Arneth, A.; Monson, R.K.; Schurgers, G.; Niinemets, Ü.; Palmer, P.I. Why are estimates of global terrestrial isoprene emissions so similar (and why is this not so for monoterpenes)? *Atmos. Chem. Phys.* **2008**, *8*, 4605–4620. [CrossRef]

22. Calfapietra, C.; Fares, S.; Manes, F.; Morani, A.; Sgrigna, G.; Loreto, F. Role of biogenic volatile organic compounds (BVOC) emitted by urban trees on ozone concentration in cities: A review. *Environ. Pollut.* **2013**, *183*, 71–80. [CrossRef] [PubMed]

23. Chameides, W.L.; Lindsay, R.W.; Richardson, J. The Role of Biogenic Hydrocarbons in Urban Photochemical Smog: Atlanta as a Case Study. *Science* **1988**, *241*, 1473–1475. [CrossRef]

24. Ryerson, T.B.; Trainer, M.; Holloway, J.S.; Parrish, D.D.; Huey, L.G.; Sueper, D.T.; Frost, G.J.; Donnelly, S.G.; Schauffler, S.; Atlas, E.L.; et al. Observations of Ozone Formation in Power Plant Plumes and Implications for Ozone Control Strategies. *Science* **2001**, *292*, 719. [CrossRef] [PubMed]

25. Kleinman, L.I.; Daum, P.H.; Imre, D.; Lee, Y.-N.; Nunnermacker, L.J.; Springston, S.R.; Weinstein-Lloyd, J.; Rudolph, J. Ozone production rate and hydrocarbon reactivity in 5 urban areas: A cause of high ozone concentration in Houston. *Geophys. Res. Lett.* **2002**, *29*, 105-1–105-4. [CrossRef]

26. Fares, S.; Barta, C.; Ederli, L.; Ferranti, F.; Pasqualini, S.; Reale, L.; Brilli, F.; Tricoli, D.; Loreto, F. Impact of high ozone on isoprene emission and some anatomical and physiological parameters of developing Populus alba leaves directly or indirectly exposed to the pollutant. *Physiol. Plant.* **2006**, *128*, 456–465. [CrossRef]

27. Wittig, V.E.; Ainsworth, E.A.; Naidu, S.L.; Karnoski, D.F.; Long, S.P. Quantifying the impact of current and future tropospheric ozone on tree biomass, growth, physiology and biochemistry: A quantitative meta-analysis. *Glob. Chang. Biol.* **2009**, *15*, 396–424. [CrossRef]

28. Kurpius, M.R.; Goldstein, A.H. Gas-phase chemistry dominates O3 loss to a forest, implying a source of aerosols and hydroxyl radicals to the atmosphere. *Geophys. Res. Lett.* **2003**, *30*, 1371. [CrossRef]

29. Agyei, T.; Juráň, S.; Kwakye, K.O.; Šigut, L.; Urban, O.; Marek, M.V. The impact of drought on total ozone flux in a mountain Norway spruce forest. *J. For. Sci.* **2020**, *66*, 280–287. [CrossRef]

30. Ashmore, M.R. Assessing the future global impacts of ozone on vegetation. *Plant Cell Environ.* **2005**, *28*, 949–964. [CrossRef]

31. Sitch, S.; Cox, P.M.; Collins, W.J.; Huntingford, C. Indirect radiative forcing of climate change through ozone effects on the land-carbon sink. *Nature* **2007**, *448*, 791–794. [CrossRef] [PubMed]

32. Hoffmann, T.; Odum, J.R.; Bowman, F.; Collins, D.; Klockow, D.; Flagan, R.C.; Seinfeld, J.H. Formation of organic aerosols from the oxidation of biogenic hydrocarbons. *J. Atmos. Chem.* **1997**, *26*, 189–222. [CrossRef]

33. O'Dowd, C.D.; Jimenez, J.L.; Bahreini, R.; Flagan, R.C.; Seinfeld, J.H.; Hämeri, K.; Pirjola, L.; Kulmala, M.; Jennings, S.G.; Hoffmann, T. Marine aerosol formation from biogenic iodine emissions. *Nature* **2002**, *417*, 497–501. [CrossRef]

34. Claeys, M.; Graham, B.; Vas, G.; Wang, W.; Vermeylen, R.; Pashynska, V.; Cafmeyer, J.; Guyon, P.; Andreae, M.O.; Artaxo, P.; et al. Formation of secondary organic aerosols through photooxidation of isoprene. *Science* **2004**, *303*, 1173–1176. [CrossRef] [PubMed]

35. Kulmala, M.; Suni, T.; Lehtinen, K.E.J.; Dal Maso, M.; Boy, M.; Reissell, A.; Rannik, Û.; Aalto, P.; Keronen, P.; Hakola, H.; et al. A new feedback mechanism linking forests, aerosols, and climate. *Atmos. Chem. Phys.* **2004**, *4*, 557–562. [CrossRef]

36. VanReken, T.M.; Greenberg, J.P.; Harley, P.C.; Guenther, A.B.; Smith, J.N. Direct measurement of particle formation and growth from the oxidation of biogenic emissions. *Atmos. Chem. Phys.* **2006**, *6*, 4403–4413. [CrossRef]

37. Spracklen, D.V.; Bonn, B.; Carslaw, K.S. Boreal forests, aerosols and the impacts on clouds and climate. *Philos. Trans. R. Soc. A* **2008**, *366*, 4613–4626. [CrossRef]

38. Paasonen, P.; Asmi, A.; Petäjä, T.; Kajos, M.K.; Äijälä, M.; Junninen, H.; Holst, T.; Abbatt, J.P.D.; Arneth, A.; Birmili, W.; et al. Warming-induced increase in aerosol number concentration likely to moderate climate change. *Nat. Geosci.* **2013**, *6*, 438–442. [CrossRef]

39. Ehn, M.; Thornton, J.A.; Kleist, E.; Sipilä, M.; Junninen, H.; Pullinen, I.; Springer, M.; Rubach, F.; Tillmann, R.; Lee, B.; et al. A large source of low-volatility secondary organic aerosol. *Nature* **2014**, *506*, 476–479. [CrossRef]

40. Boucher, O.; Randall, P.D.; Artaxo, C.; Bretherton, G.; Feingold, P.; Forster, V.-M.; Kerminen, Y.; Kondo, H.; Liao, U.; Lohmann, P.; et al. 2013: Clouds and Aerosols. In *Climate Change 2013: The Physical Science Basis. Contribution of Working Group I to the Fifth Assessment Report of the Intergovernmental Panel on Climate Change*; Stocker, T.F., Qin, D., Plattner, G.-K., Tignor, M., Allen, S.K., Boschung, J., Nauels, A., Xia, Y., Bex, V., Midgley, P.M., Eds.; Cambridge University Press: Cambridge, UK; New York, NY, USA, 2013.

41. Vedel-Petersen, I.; Schollert, M.; Nymand, J.; Rinnan, R. Volatile organic compound emission profiles of four common arctic Plants. *Atmos. Environ.* **2015**, *120*, 117–126. [CrossRef]

42. Karlsson, T.; Rinnan, R.; Holst, T. Variability of BVOC Emissions from Commercially Used Willow (Salix spp.) Varieties. *Atmosphere* **2020**, *11*, 356. [CrossRef]

43. Owen, S.M.; Boissard, C.; Hewitt, C.N. Volatile organic compounds (VOCs) emitted from 40 Mediterranean plant species: VOC speciation and extrapolation to habitat scale. *Atmos. Environ.* **2001**, *35*, 5393–5409. [CrossRef]

44. Olofsson, M.; Ekolausson, B.; Jensen, N.; Langer, S.; Ljungström, E. The flux of isoprene from a willow coppice plantation and the effect on local air quality. *Atmos. Environ.* **2005**, *39*, 2061–2070. [CrossRef]

45. Niinemets, Ü.; Copolovici, L.; Hüve, K. High within-canopy variation in isoprene emission potentials in temperate trees: Implications for predicting canopy-scale isoprene fluxes. *J. Geophys. Res.* **2010**, *115*, G04029. [CrossRef]

46. Persson, Y.; Schurgers, G.; Ekberg, A.; Holst, T. Effects of intra-genotypic variation, variance with height and time of season on BVOC emissions. *Meteorol. Z.* **2016**, *25*, 377–388. [CrossRef]

47. Alexandersson, H.; Eggertsson Karlström, C. *Temperaturen och nederbörden i Sverige 1961–90: Referensnormaler—utgåva 2. Meteorologi 99*; Swedish Meteorological and Hydrological Institute: Norrköping, Sweden, 2001. (In Swedish)

48. SGU, Geology Survey of Sweden. Available online: http://maps-test.sgu.se:8080/TestSguMapViewer2/kartvisare-lerhaltskarta-sv.html (accessed on 7 March 2019).

49. Haapanala, S.; Ekberg, A.; Hakola, A.; Tarvainen, V.; Rinne, J.; Hellén, H.; Arneth, A. Mountain birch—Potentially large source of sesquiterpenes into high latitude atmosphere. *Biogeosciences* **2009**, *6*, 2709–2718. [CrossRef]

50. van Meeningen, Y.; Wang, M.; Karlsson, T.; Seifert, A.; Schurgers, G.; Rinnan, R.; Holst, T. Isoprenoid emission variation of Norway spruce across a European latitudinal transect. *Atmos. Environ.* **2017**, *170*, 45–57. [CrossRef]

51. Wang, M.; Schurgers, G.; Arneth, A.; Ekberg, A.; Holst, T. Seasonal variation in biogenic volatile organic compound (BVOC) emissions from Norway spruce in a Swedish boreal forest. *Boreal Environ. Res.* **2017**, *22*, 353–367.

52. van Meeningen, Y.; Schurgers, G.; Rinnan, R.; Holst, T. Isoprenoid emission response to changing light conditions of English oak, European beech and Norway spruce. *Biogeosciences* **2017**, *14*, 4045–4060. [CrossRef]

53. Lindwall, F.; Svendsen, S.S.; Nielsen, C.S.; Michelsen, A.; Rinnan, R. Warming in-creases isoprene emissions from an arctic fen. *Sci. Total Environ.* **2016**, *553*, 297–304. [CrossRef] [PubMed]

54. Ortega, J.; Helmig, D. Approaches for quantifying reactive and low-volatility biogenic organic compound emissions by vegetation enclosure techniques—Part A. *Chemosphere* **2008**, *72*, 343–364. [CrossRef]

55. Guenther, A.B.; Zimmerman, P.; Harley, P.C.; Monson, R.K.; Fall, R. Isoprene and monoterpene emission rate variability: Model evaluations and sensitivity analyses. *J. Geophys. Res.* **1993**, *98*, 12609–12617. [CrossRef]

56. Helmig, D.; Ortega, J.; Duhl, T.; Tanner, D.; Guenther, A.; Harley, P.; Wiedinmyer, C.; Milford, J.; Sakulyanontvittaya, T. Sesquiterpene Emissions from Pine Trees—Identifications, Emission Rates and Flux Estimates for the Contiguous United States. *Environ. Sci. Technol.* **2007**, *41*, 1545–1553. [CrossRef] [PubMed]

57. Niinemets, Ü.; Sun, Z.; Talts, E. Controls of the quantum yield and saturation light of isoprene emission in different-aged aspen leaves. *Plant Cell Environ.* **2015**, *38*, 2707–2720. [CrossRef] [PubMed]

58. Owen, S.M.; Hewitt, C.N. Extrapolating branch enclosure measurements to estimates of regional scale biogenic VOC fluxes in the north-western Mediterranean basin. *J. Geophys. Res.* **2000**, *105*, 11573–11583. [CrossRef]

59. Morrison, E.C.; Drewer, J.; Heal, M.R. A comparison of isoprene and monoterpene emission rates from the perennial bioenergy crops short-rotation coppice willow and Miscanthus and the annual arable crops wheat and oilseed rape. *GCB Bioenergy* **2016**, *8*, 211–225. [CrossRef]

60. Monson, R.K.; Jaeger, C.H.; Adams, W.; Driggers, E.; Silver, G.; Fall, R. Relationships among isoprene emission rate, photosynthesis rate, and isoprene synthase activity, as influenced by temperature. *Plant Physiol.* **1992**, *92*, 1175–1180. [CrossRef]

61. Kuzma, J.; Fall, R. Leaf isoprene emission rate is dependent on leaf development and the level of isoprene synthase. *Plant Physiol.* **1993**, *101*, 435–440. [CrossRef]

62. Monson, R.K.; Harley, P.C.; Litvak, M.E.; Wildermuth, M.; Guenther, A.B.; Zimmerman, P.R.; Fall, R. Environmental and developmental controls over the seasonal pattern of isoprene emission from aspen leaves. *Oecologia* **1994**, *99*, 260–270. [CrossRef]

63. Schnitzler, J.-P.; Lehning, A.; Steinbrecher, R. Seasonal Pattern of Isoprene Synthase Activity in Quercus robur Leaves and its Significance or Modeling Isoprene Emission Rates. *Bot. Acta* **1997**, *110*, 240–243. [CrossRef]

64. Toome, M.; Randjärv, P.; Copolovici, L.; Niinemets, Ü.; Heinsoo, K.; Luik, A.; Noe, S.M. Leaf rust induced volatile organic compounds signalling in willow during the infection. *Planta* **2010**, *232*, 235–243. [CrossRef]

65. Jiang, Y.; Ye, J.; Veromann, L.-L.; Niinemets, Ü. Scaling of photosynthesis and constitutive and induced volatile emissions with severity of leaf infection by rust fungus (Melampsora larici-populina) in Populus balsamifera var. suaveolens. *Tree Physiol.* **2016**, *36*, 856–872. [CrossRef] [PubMed]

66. Sharkey, T.D.; Loreto, F.; Delwiche, C.F. High carbon dioxide and sun/shade effects on isoprene emission from oak and aspen tree leaves. *Plant Cell Environ.* **1991**, *14*, 333–338. [CrossRef]

67. Lerdau, M.; Throop, H.L. Sources of variability in isoprene emission and photosynthesis in two species of tropical wet forest trees. *Biotropica* **2000**, *32*, 670–676. [CrossRef]

68. Monson, R.K.; Fall, R. Isoprene emission from aspen leaves. *Plant Physiol.* **1989**, *90*, 267–274. [CrossRef] [PubMed]

69. Guenther, A.B.; Monson, R.K.; Fall, R. Isoprene and monoterpene emission rate variability: Observations with eucalyptus and emission rate algorithm development. *J. Geophys. Res.* **1991**, *96*, 10799–10808. [CrossRef]

70. Sharkey, T.D.; Monson, R.K. Isoprene research—60 years later, the biology is still enigmatic. *Plant Cell Environ.* **2017**, *40*, 1671–1678. [CrossRef]

71. Simin, T.; Tang, J.; Holst, T.; Rinnan, R. Volatile organic compound emission in tundra shrubs—Dependence on species characteristics and the near-surface environment. *Environ. Exp. Bot.* **2021**, *184*, 104387. [CrossRef]

72. Niinemets, Ü.; Tenhunen, J.D.; Harley, P.C.; Steinbrecher, R. A model of isoprene emission based on energetic requirements for isoprene synthesis and leaf photosynthetic properties for Liquidambar and Quercus. *Plant Cell Environ.* **1999**, *22*, 1319–1335. [CrossRef]

73. Kenzo, T.; Ichie, T.; Watanabe, Y.; Yoneda, R.; Ninomiya, I.; Koike, T. Changes in photosynthesis and leaf characteristics with tree height in five dipterocarp species in a tropical rain forest. *Tree Physiol.* **2006**, *26*, 865–873. [CrossRef] [PubMed]

74. Kosugi, Y.; Takanashi, S.; Yokoyama, N.; Philip, E.; Kamakura, M. Vertical variation in leaf gas exchange parameters for a Southeast Asian tropical rainforest in Peninsular Malaysia. *J. Plant Res.* **2012**, *125*, 735–748. [CrossRef] [PubMed]

75. Juráň, S.; Pallozzi, E.; Guidolotti, G.; Fares, S.; Šigut, L.; Calfapietra, C.; Alivernini, A.; Savi, F.; Večeřová, K.; Křůmal, K.; et al. Fluxes of biogenic volatile organic compounds above temperate Norway spruce forest of the Czech Republic. *Agric. For. Meteorol.* **2017**, *232*, 500–513. [CrossRef]

76. Guidolotti, G.; Calfapietra, C.; Loreto, F. The relationship between isoprene emission, CO_2 assimilation and water use efficiency across a range of poplar genotypes. *Physiol. Plant.* **2011**, *142*, 297–304. [CrossRef]

77. Tingey, D.T.; Manning, M.; Grothaus, L.C.; Burns, W.F. The influence of light and temperature on isoprene emission rates from live oak. *Physiol. Plant.* **1979**, *47*, 112–118. [CrossRef]

78. Llusià, J.; Peñuelas, J. Seasonal patterns of terpene content and emission from seven Mediterranean woody species in field conditions. *Am. J. Bot.* **2000**, *87*, 133–140. [CrossRef] [PubMed]

79. Kesselmeier, J.; Ciccioli, P.; Kuhn, U.; Stefani, P.; Biesenthal, T.; Rottenberger, S.; Wolf, A.; Vitullo, M.; Valentini, R.; Nobre, A.; et al. Volatile organic compound emissions in relation to plant carbon fixation and the terrestrial carbon budget. *Glob. Biogeochem. Cycles* **2002**, *16*, 1126. [CrossRef]

80. Bracho-Nunez, A.; Knothe, N.M.; Welter, S.; Staudt, M.; Costa, W.R.; Liberato, M.A.R.; Piedade, M.T.F.; Kesselmeier, J. Leaf level emissions of volatile organic compounds (VOC) from some Amazonian and Mediterranean plants. *Biogeosciences* **2013**, *10*, 5855–5873. [CrossRef]

81. Loreto, F.; Sharkey, T.D. A gas-exchange study of photosynthesis and isoprene emission in *Quercus rubra* L. *Planta* **1990**, *182*, 523–531. [CrossRef]

82. Larcher, W. Carbon Utilization and Dry Matter Production. In *Physiological Plant Ecology: Ecophysiology and Stress Physiology of Functional Groups*, 4th ed.; Springer: Berlin/Heidelberg, Germany; New York, NY, USA, 2003; pp. 69–184.

83. Winer, A.M.; Arey, J.; Atkinson, R.; Aschmann, S.M.; Long, W.D.; Morrison, C.L.; Olszyk, D.M. Emission rates of organics from vegetation in California's central valley. *Atmos. Environ.* **1992**, *26*, 2647–2659. [CrossRef]

84. König, G.; Brunda, M.; Puxbaum, H.; Hewitt, C.N.; Duckham, S.C.; Rudolph, J. Relative contribution of oxygenated hydrocarbons to the total biogenic VOC emissions of selected mid-European agricultural and natural plant species. *Atmos. Environ.* **1995**, *29*, 861–874. [CrossRef]

85. Karl, M.; Guenther, A.; Köble, R.; Leip, A.; Seufert, G. A new European plantspecific emission inventory of biogenic volatile organic compounds for use in atmospheric transport models. *Biogeosciences* **2009**, *6*, 1059–1087. [CrossRef]

86. Roberts, J.M.; Williams, J.; Baumann, K.; Buhr, M.P.; Goldan, P.D.; Holloway, J.; Hubler, G.; Kuster, W.C.; McKeen, S.A.; Ryerson, T.B.; et al. Measurements of PAN, PPN, MPAN made during the 1994 and 1995 Nashville Intensives of the Southern Oxidant Study: Implications for regional ozone production from biogenic hydrocarbons. *J. Geophys. Res.* **1998**, *103*, 22473–22490. [CrossRef]

87. Wang, K.-Y.; Shallcross, D.E. Modelling terrestrial biogenic isoprene fluxes and their potential impact on global chemical species using a coupled LSM-CTM model. *Atmos. Environ.* **2000**, *34*, 2909–2925. [CrossRef]

88. Watson, L.A.; Wang, K.-Y.; Paul, H.; Shallcross, D.E. The potential impact of biogenic emissions of isoprene on urban chemistry in the United Kingdom. *Atmos. Sci. Lett.* **2006**, *7*, 96–100. [CrossRef]

89. Hakola, H.; Rinne, J.; Laurila, T. The VOC emission rates of boreal deciduous trees. In *Biogenic VOC Emissions and Photochemistry in the Boreal Regions of Europe-Biphorep*; European Commission: Brussels, Belgium, 1999.

90. Staudt, M.; Seufert, G. Light-dependent emission of monoterpenes by Holm oak (Quercus ibex L.). *Naturwissenschaften* **1995**, *82*, 89–92. [CrossRef]

91. Kesselmeier, J.; Schäfer, L.; Ciccioli, P.; Brancaleoni, E.; Cecinato, A.; Frattoni, M.; Foster, P.; Jacob, V.; Denis, J.; Fugit, J.-L.; et al. Emission of monoterpenes and isoprene from a Mediterranean oak species Quercus ilex L. measured within the BEMA (Biogenic Emissions in the Mediterranean Area) project. *Atmos. Environ.* **1996**, *30*, 1841–1850. [CrossRef]

92. Peñuelas, J.; Llusià, J. Short-term responses of terpene emission rates to experimental changes of PFD in Pinus halepensis and Quercus ilex in summer field conditions. *Environ. Exp. Bot.* **1999**, *42*, 61–68. [CrossRef]

93. Loreto, F.; Forster, A.; Durr, M.; Csiky, O.; Seufert, G. On the monoterpene emission under heat stress and on the increased thermotolerance of leaves of *Quercus ilex* L. fumigated with selected monoterpenes. *Plant Cell Environ.* **1998**, *21*, 101–107. [CrossRef]

94. Paré, P.W.; Tumlinson, J.H. Plant volatiles as a defense against insect herbivores. *Plant Physiol.* **1999**, *121*, 325–332. [CrossRef]

95. Delfine, S.; Csiky, O.; Seufert, G.; Loreto, F. Fumigation with exogenous monoterpenes of a non-isoprenoid-emitting oak (Quercus suber): Monoterpene acquisition, translocation, and effect on the photosynthetic properties at high temperatures. *New Phytol.* **2000**, *146*, 27–36. [CrossRef]

96. Peñuelas, J.; Llusià, J. Linking photorespiration, monoterpenes and thermotolerance in Quercus. *New Phytol.* **2002**, *155*, 227–237. [CrossRef]

97. Copolovici, L.; Kännaste, A.; Pazouki, L.; Niinemets, Ü. Emissions of green leaf volatiles and terpenoids from Solanum lycopersicum are quantitatively related to the severity of cold and heat shock treatments. *J. Plant Physiol.* **2012**, *169*, 664–672. [CrossRef]

98. Palmer-Young, E.C.; Veit, D.; Gershenzon, J.; Schuman, M.C. The Sesquiterpenes (E)-ß-Farnesene and (E)-α-Bergamotene Quench Ozone but Fail to Protect the Wild Tobacco Nicotiana attenuata from Ozone, UVB, and Drought Stresses. *PLoS ONE* **2015**, *10*, e0127296.

99. Pazouki, L.; Kanagendran, A.; Li, S.; Kännaste, A.; Memari, H.R.; Bichele, R.; Niinemets, Ü. Mono- and sesquiterpene release from tomato (Solanum lycopersicum) leaves upon mild and severe heat stress and through recovery: From gene expression to emission responses. *Environ. Exp. Bot.* **2016**, *132*, 1–15. [CrossRef]

100. Tiiva, P.; Häikiö, E.; Kasurinen, A. Impact of warming, moderate nitrogen addition and bark herbivory on BVOC emissions and growth of Scots pine (Pinus sylvestris L.) seedlings. *Tree Physiol.* **2018**, *38*, 1461–1475. [CrossRef] [PubMed]

101. Hildebrand, D.F. Lipoxygenases. *Physiol. Plant.* **1989**, *76*, 249–253. [CrossRef]

102. Andersen, R.A.; Hamilton-Kemp, T.R.; Hildebrand, D.F.; McCracken, C.T.; Collins, R.W.; Fleming, P.D. Structure-Antifungal Activity Relationships among Volatile C6 and C9 Aliphatic Aldehydes, Ketones, and Alcohols. *J. Agric. Food Chem.* **1994**, *42*, 1563–1568. [CrossRef]

103. Wildt, J.; Kobel, K.; Schuh-Thomas, G.; Heiden, A. Emissions of Oxygenated Volatile Organic Compounds from Plants Part II: Emissions of Saturated Aldehydes. *J. Atmos. Chem.* **2003**, *45*, 173–196. [CrossRef]

104. Misztal, P.K.; Hewitt, C.N.; Wildt, J.; Blande, J.D.; Eller, A.; Fares, S.; Gentner, D.; Gilman, J.; Graus, M.; Greenberg, J.; et al. Atmospheric benzenoid emissions from plants rival those from fossil fuels. *Sci. Rep.* **2015**, *5*, 12064. [CrossRef]

105. Arimura, G.; Huber, D.P.; Bohlmann, J. Forest tent caterpillars (Malacosoma disstria) induce local and systemic diurnal emissions of terpenoid volatiles in hybrid poplar (Populus trichocarpa x deltoides): cDNA cloning, functional characterization, and patterns of gene expression of (−)-germacrene D synthase, PtdTPS1. *Plant J.* **2004**, *37*, 603–616. [PubMed]

106. Kleist, E.; Mentel, T.F.; Andres, S.; Bohne, A.; Folkers, A.; Kiendler-Scharr, A.; Rudich, Y.; Springer, M.; Tillmann, R.; Wildt, J. Irreversible impacts of heat on the emissions of monoterpenes, sesquiterpenes, phenolic BVOC and green leaf volatiles from several tree species. *Biogeosciences* **2012**, *9*, 5111–5123. [CrossRef]

107. Hakola, H.; Rinne, J.; Laurila, T. The hydrocarbon emission rates of tea-leafed willow (Salix phylicifolia), silver birch (Betula pendula) and European aspen (Populus tremula). *Atmos. Environ.* **1998**, *32*, 1825–1833. [CrossRef]

108. Copeland, N.; Cape, J.N.; Heal, M.R. Volatile organic compound emissions from Miscanthus and short rotation coppice willow bioenergy crops. *Atmos. Environ.* **2012**, *60*, 327–335. [CrossRef]

109. Peräkylä, O.; Vogt, M.; Tikkanen, O.P.; Laurila, T.; Kajos, M.K.; Rantala, P.A.; Patokoski, J.; Aalto, J.; Yli-Juuti, T.; Ehn, M.; et al. Monoterpenes oxidation capacity and rate over a boreal forest: Temporal variation and connection to growth of newly formed particles. *Boreal Environ. Res.* **2014**, *19*, 293–310.